

Modeling False Data Injection Attacks on Integrated Electricity-Gas Systems

Rong-Peng Liu, *Member, IEEE*, Xiaozhe Wang, *Senior Member, IEEE*, Zuyi Li, *Senior Member, IEEE*, and Rawad Zgheib

Abstract—Integrated electricity-gas systems (IEGSs) rely heavily on communication systems and are vulnerable to cyberattacks. In order to gain insights into intruders’ behavior and design tailored detection and mitigation methods, this paper studies the modeling of false data injection attacks (FDIAs) on IEGSs. First, we introduce a tailored static state estimation model and bad data detection method for IEGSs. Then, we develop FDIAs on IEGSs with complete network topology and parameter information and give conditions that ensure the stealthiness of these FDIAs. Next, we develop FDIAs on IEGSs when intruders have only local network topology and parameter information of an IEGS. Lastly, we explore FDIAs on IEGSs when intruders have only local network topology information of an IEGS, and mathematically prove the existence of (stealthy) FDIAs, specifically targeting gas compressors. Simulation results validate the effectiveness of the proposed FDIAs on IEGSs with both complete and incomplete network information.

Index Terms—Cybersecurity, false data injection attacks, incomplete network information, integrated electricity-gas systems, state estimation.

NOMENCLATURE

\mathcal{G}_w	Set of gas wells.
$\mathcal{P}_d/\mathcal{G}_d$	Set of power/gas loads.
$\mathcal{P}_g/\mathcal{G}_g$	Set of coal-fired/gas-fired power generators.
$\mathcal{P}_l/\mathcal{G}_l/\mathcal{G}_c$	Set of power transmission lines/gas passive pipelines/gas compressors.
$\mathcal{P}_n/\mathcal{G}_n$	Set of power buses/gas nodes.
\mathcal{P}'_n	Set of the power buses equipped with phasor measurement units (PMUs).
C_{ij}^{\max}	Transmission limit of gas compressor $\{i, j\}$.
G_i^{\min}/G_i^{\max}	Minimum/maximum gas injection at gas node i .
G_{ij}/B_{ij}	Conductance/susceptance of power transmission line $\{i, j\}$.
G_w^{\max}	Maximum output capacity of gas well w .
$P_d/Q_d/G_d$	Real power/reactive power/gas load d .
P_i^{\min}/P_i^{\max}	Minimum/maximum real power injection at power bus i .
Q_i^{\min}/Q_i^{\max}	Minimum/maximum reactive power injection at power bus i .
V_i^{\min}/V_i^{\max}	Minimum/maximum voltage magnitude at power bus i .
$S_{ij}^{\max}/G_{ij}^{\max}$	Transmission limit of power transmission line $\{i, j\}$ /gas passive pipeline $\{i, j\}$.

This work was supported in part by Hydro-Québec, the Institut de Valorisation des Données (IVADO), MITACS under Grant IT27493, in part by the Natural Sciences and Engineering Research Council of Canada (NSERC) under Alliance Grants ALLRP 566986-21, and in part by the Fonds de recherche du Québec – Nature et technologies (FRQNT) under Grant 334636.

R. Liu and X. Wang are with the Department of Electrical and Computer Engineering, McGill University, Montreal, QC H3A 0E9, Canada (e-mail: rpliu@eee.hku.hk/rongpeng.liu@mail.mcgill.ca; xiaozhe.wang2@mcgill.ca).

Z. Li is with the College of Electrical Engineering, Zhejiang University, Hangzhou, China, 310013 (email: lizuyi@zju.edu.cn).

R. Zgheib is with Hydro-Quebec Research Institute (IREQ) (email: zgheib.rawad2@hydroquebec.com).

W_{ij}	Weymouth constant of gas passive pipeline $\{i, j\}$.
α_{ij}	Compression ratio of gas compressor $\{i, j\}$.
γ_g	Electricity-gas conversion ratio of gas-fired power generator g .
$\Pi_i^{\min}/\Pi_i^{\max}$	Minimum/maximum nodal pressure at gas node i .
θ_i^{\max}	Maximum phase angle at power bus i .
g_{ij}/c_{ij}	Gas flow in gas passive pipeline/gas compressor ij .
g_i	Gas injection at gas node i .
g_w	Gas output of gas well w .
p_g/q_g	Real/reactive power output of power generator g .
p_{ij}/q_{ij}	Real/reactive power flow in power transmission line $\{i, j\}$.
p_i/q_i	Real/reactive power injection at power bus i .
v_i/π_i	Voltage magnitude/nodal pressure at power bus/gas node i .
θ_i	Phase angle at power bus i .
$\Delta g_{ij}/\Delta c_{ij}$	Injected false data in the gas flow measurement in gas passive pipeline/gas compressor $\{i, j\}$.
Δg_i	Injected false data in the gas injection measurement at gas node i .
$\Delta p_{ij}/\Delta q_{ij}$	Injected false data in the real/reactive power flow measurement in power transmission line $\{i, j\}$.
$\Delta p_i/\Delta q_i$	Injected false data in the real/reactive power injection measurement at power bus i .
$\Delta v_i/\Delta \pi_i$	Injected false data in the voltage magnitude/nodal pressure measurement at power bus/gas node i .
$\Delta \theta_i$	Injected false data in the phase angle measurement at power bus i .

I. INTRODUCTION

Integrated electricity-gas systems (IEGSs) have been extensively constructed to facilitate gas-fired power generation and reduce operation costs [1], [2]. Meanwhile, cyber incidents in the energy sector have rocketed [3], resulting in severe consequences [4], [5] and unveiling the vulnerability of power and gas systems to cyberattacks. Theoretically, IEGSs are vulnerable to cyberattacks due to the heavy reliance on communication systems (to maintain synchronous operation of power and gas systems). Ensuring the IEGS cybersecurity is a critical concern.

Prior research has extensively studied power system cyber-attack paradigms [6]–[8]. Fundamentally, reference [6] pointed out that power systems were vulnerable to false data injection attacks (FDIAs). These attacks can perfectly bypass bad data detection (BDD) and compromise the direct current (DC) state estimation (SE) of power systems. Reference [7] further analyzed the impact of FDIAs on alternating current (AC) SE. Reference [8] designed sequential FDIAs against state-of-charge estimations of battery energy storage systems in distribution systems. These studies promote further research on the cybersecurity of the power subsector and other energy subsectors.

Recently, cyberattacks on IEGSs have intrigued researchers’ interests [9]–[15]. Reference [9] developed FDIAs targeting the gas system in an IEGS and evaluated their impact on the interconnected power system. Reference [10] investigated FDIAs involving false gas supply information for gas-fired generators

in IEGSSs. Reference [11] explored cyberattacks on compressor stations in IEGSSs. Reference [12] proposed FDIAs on power and gas pipeline monitoring systems in an IEGS, separately, for disabling gas-fired generators and disconnecting entire IEGSSs. References [13]-[15] developed load redistribution attacks targeting the distribution system within an IEGS, FDIAs targeting an entire IEGSSs, and FDIAs on entire integrated electricity-gas-water systems, respectively. Despite significant advancements, there still exist distinct gaps in the study of *FDIAs on IEGSSs* proposed in [9]-[15]: i) the SE and BDD for an entire IEGS are not defined clearly; ii) the FDIAs on IEGSSs are developed using simplified power flow models; iii) the FDIAs on IEGSSs overlook crucial interdependency between power and gas systems within an IEGS. More details are shown in Table I.

Another challenge of designing FDIAs is that intruders may lack full knowledge of network information. Previous works [6]-[15], however, assume intruders have complete network information, i.e., network topology and parameters. In response, researchers investigated *cyberattacks on power systems (rather than IEGSSs) with incomplete network information* [16]-[22]. References [16]-[17] studied local load redistribution attacks against DC SE with incomplete network information. References [18]-[21] proposed local FDIAs on power system SE with incomplete network information. References [22] constructed blind FDIAs (without any network information) on AC SE by a geometric method. See [23] for a review of cyberattacks on power systems with incomplete network information.

To the best of our knowledge, FDIAs on IEGSSs with *incomplete network information* have never been studied, despite the fact that intruders are more likely to have only local network information of an IEGS in real world. Existing FDIA paradigms on power systems with either complete or incomplete network information cannot be trivially extended to IEGSSs due to i) significant differences between power and gas infrastructures, leading to distinct mathematical formulations, and ii) the interdependency between power and gas systems in an IEGS.

This work addresses these critical research gaps and studies FDIAs on *transmission-level IEGSSs*. Table I summarizes the major differences between this work and previous works. In essence, the contributions of this work are twofold:

1) *FDIAs on IEGSSs with complete network information*: We develop the static IEGS SE and a tailored BDD method to detect bad data during the SE. Then, we propose FDIAs on IEGSSs with complete network information and establish conditions to ensure their stealthiness. Particularly, the FDIAs are developed based on an AC power flow model [7] and consider the cyberattack interdependency (CAI)^{#b} (see Table I) in an entire IEGS, distinguishing them from those in previous works [9]-[15] that adopt linearized power flow models and overlook the CAI in IEGSSs. In addition, we emphasize the critical role of the CAI and explain why an intruder cannot directly launch the FDIAs designed for pure power systems [6]-[8], [16]-[22] in the power subsystem of an IEGSSs without considering the gas subsystem.

2) *FDIAs on IEGSSs with incomplete network information*: For the first time, we develop FDIAs on IEGSSs when intruders have only local network (topology and parameter) information of an IEGS and give conditions to ensure the stealthiness of

these FDIAs. Furthermore, for the first time, we explore FDIAs on IEGSSs when intruders have only local network topology information of an IEGS, and mathematically prove that: i) topology-only (stealthy) attacks on the power system in an IEGS do not exist in general, and ii) topology-only (stealthy) attacks on the gas system in an IEGS exist, specifically targeting gas compressors. Test results show the effectiveness of the proposed FDIAs on IEGSSs with complete/incomplete information.

The rest of this paper is organized as follows. Section II introduces IEGS SE. Section III designs FDIAs on IEGSSs with complete network information. Section IV studies FDIAs on IEGSSs with incomplete network information. Section V presents testing results. Section VI draws conclusions.

TABLE I
COMPARISON WITH EXISTING WORKS REGARDING CYBERATTACKS ON IEGSS

Ref.	Type of attack	Attack target	PF model ^{#a}	CAI ^{#b}	Network information ^{#c}
[9]	FDIAs	Gas systems in IEGSSs	DC	×	C
[10]	FDIAs	Gas systems in IEGSSs	DC	×	C
[11]	Cyberattacks	Gas systems in IEGSSs	DC	×	C
[12]	FDIAs	Separate power and gas systems in an IEGS	DC	×	C
[13]	LR attacks	Power systems in IEGSSs	LDF	×	C
[14]	FDIAs	Entire IEGSSs	DC	×	C
[15]	FDIAs	Entire integrated electricity-gas-water systems	DC	×	C
This work	FDIAs	Entire IEGSSs	AC	✓	C and IC

#a: Power flow (PF) models: DC, AC, or linearized DistFlow (LDF) power flow model.
#b: Cyberattack interdependency (CAI), i.e., if a cyberattack considers coupling constraints, e.g., the gas supply to gas-fired power generators.
#c: Intruders are assumed to have complete/incomplete (C/IC) network information.

II. STATE ESTIMATION AND BAD DATA DETECTION

In this section, we begin with a review of the SE of power systems and FDIAs targeting power systems. Subsequently, we develop a static SE model designed specifically for IEGSSs and a tailored method for identifying bad data during the SE of IEGSSs. Before proceeding, we clarify the scope of this work.

1) This work studies FDIAs on (connected) *transmission-level IEGSSs*, as gas systems may be more commonly coupled to power systems on the transmission level [24]. For the power system in an IEGS, we adopt an AC power flow model [18]. For the gas system in an IEGS, we adopt a Weymouth equation [9], [12], which is broadly adopted to model the gas flow in transmission-level gas passive pipelines.

2) This work aims at steady-state IEGSSs [9]-[12]. The dynamics of IEGSSs, especially after FDIAs, are another important research topic but are beyond the scope of this paper.

3) This work assumes that IEGSSs are observable (from IEGS operators' perspective). Detailed discussions are in Section III.

4) This work assumes that intruders can get access to (at least local) measurements in an IEGS and manage to inject false data into these measurements [9]-[12].

5) In this paper, a compressor refers to the gas pipeline that is driven by a compressor (also known as a gas active pipeline). Without loss of generality, this work considers both simplified and detailed compressor models [25].

Notations: This paper utilizes i) regular lowercase or uppercase letters to denote scalars; ii) bold lowercase and uppercase letters to denote vectors and matrices, respectively; iii) calligraphic/hollow uppercase letters to denote sets. Vectors are col-

umn vectors, whose transpose is denoted by superscript \top . The terms ‘‘FDIAs on power systems/gas systems/IEGSs’’ denotes ‘‘FDIAs targeting the SE of power systems/gas system/IEGSs’’.

A. Power System SE, BDD, and FDIAs: A Preliminary

Power system measurements and state variables satisfy

$$\mathbf{z}^p = \mathbf{h}^p(\mathbf{x}^p) + \mathbf{e}^p. \quad (1)$$

$\mathbf{z}^p = \text{col}(p_i, q_i, P_{ij}, q_{ij}, v_i, \theta_i), i \in \mathcal{P}_n, \{i, j\} \in \mathcal{P}_l, i' \in \mathcal{P}'_n$, refers to the vector of measurements in a power system, i.e., real and reactive power injections, real and reactive power flows, voltage magnitudes, and the phase angles of the buses equipped with PMUs. $\mathbf{x}^p = \text{col}(v_i, \theta_i), i \in \mathcal{P}_n$, denotes the vector of state variables in a power system, i.e., voltage magnitudes and phase angles. $\text{col}(\mathbf{a}, \mathbf{b}, \mathbf{c}) = [\mathbf{a}^\top, \mathbf{b}, \mathbf{c}^\top]^\top$. $\mathbf{h}^p(\cdot)$ is the vector of functions that map power system state variables into corresponding measurements. Please refer to (B.1)-(B.4) in the Appendix for detailed formulations of the nontrivial part of $\mathbf{h}^p(\cdot)$. (The trivial part of $\mathbf{h}^p(\cdot)$ refers to identity mappings of v_i and $\theta_i, i \in \mathcal{P}_n, i' \in \mathcal{P}'_n$.) The vector of measurement errors \mathbf{e}^p is assumed to follow $\mathcal{N}(0, \mathbf{E}^p)$. By using measurements \mathbf{z}^p , system operators can estimate power system states (i.e., power system SE [7]) via

$$\hat{\mathbf{x}}^p = \arg \min_{\mathbf{x}^p} (\mathbf{z}^p - \mathbf{h}^p(\mathbf{x}^p))^\top \cdot (\mathbf{E}^p)^{-1} \cdot (\mathbf{z}^p - \mathbf{h}^p(\mathbf{x}^p)), \quad (2)$$

where $\hat{\mathbf{x}}^p$ is the vector of estimated power system states. Previous works assume power systems are observable [6]-[22].

However, power system measurements may contain bad data due to communication noises and even malicious data, affecting the quality of SE [7]. BDD is capable of detecting bad data by checking the residuals \mathbf{r}^p [7],

$$\mathbf{r}^p = \mathbf{z}^p - \mathbf{h}^p(\hat{\mathbf{x}}^p). \quad (3)$$

If $\|\mathbf{r}^p\| > \tau^p$, there exist bad data in \mathbf{z}^p , where τ^p is a predefined threshold and $\|\cdot\|$ denotes the l_2 -norm.

Unfortunately, previous works [7], [19] show that FDIAs can bypass BDD by injecting well-designed false data into power system measurements, provided that i) the true measurements \mathbf{z}^p can pass BDD, ii) intruders have full knowledge of network information $\mathbf{h}^p(\cdot)$, iii) intruders can derive or have access to all measurements \mathbf{z}^p , and iv) intruders have the same estimated states $\hat{\mathbf{x}}^p$ as those estimated by power system operators. Although the last condition is hard to check in theory, it is typically considered to be true in previous works [7], [19]. Let $\mathbf{z}_{\text{bad}}^p = \mathbf{z}^p + \Delta\mathbf{z}^p$ and $\mathbf{x}_{\text{bad}}^p = \hat{\mathbf{x}}^p + \Delta\mathbf{x}^p$. $\Delta\mathbf{z}^p = \text{col}(\Delta p_i, \Delta q_i, \Delta P_{ij}, \Delta q_{ij}, \Delta v_i, \Delta \theta_i), i \in \mathcal{P}_n, \{i, j\} \in \mathcal{P}_l, i' \in \mathcal{P}'_n$, is the vector of injected false data, $\mathbf{z}_{\text{bad}}^p$ is the vector of falsified measurements, $\Delta\mathbf{x}^p = \text{col}(\Delta v_i, \Delta \theta_i), i \in \mathcal{P}_n$, is the vector of the variations in estimated states after the attack, and $\mathbf{x}_{\text{bad}}^p$ is the vector of estimated states with falsified measurements $\mathbf{z}_{\text{bad}}^p$ (after FDIAs). We have

$$\begin{aligned} \|\mathbf{r}_{\text{bad}}^p\| &= \|\mathbf{z}_{\text{bad}}^p - \mathbf{h}^p(\mathbf{x}_{\text{bad}}^p)\| \\ &= \|\mathbf{z}^p + \Delta\mathbf{z}^p - \mathbf{h}^p(\hat{\mathbf{x}}^p + \Delta\mathbf{x}^p)\| \\ &= \|\mathbf{z}^p - \mathbf{h}^p(\hat{\mathbf{x}}^p) + \Delta\mathbf{z}^p - \mathbf{h}^p(\hat{\mathbf{x}}^p + \Delta\mathbf{x}^p) + \mathbf{h}^p(\hat{\mathbf{x}}^p)\|, \end{aligned} \quad (4)$$

where $\mathbf{r}_{\text{bad}}^p$ is the vector of residuals. If the last three terms in the last row of (4) satisfy

$$\Delta\mathbf{z}^p = \mathbf{h}^p(\hat{\mathbf{x}}^p + \Delta\mathbf{x}^p) - \mathbf{h}^p(\hat{\mathbf{x}}^p), \quad (5)$$

$\|\mathbf{r}_{\text{bad}}^p\| = \|\mathbf{r}^p\| \leq \tau^p$. Namely, the FDIA $\Delta\mathbf{z}^p$ designed based on (5) can bypass BDD and compromise power systems *stealthily*.

B. Gas System SE

This subsection develops gas system SE. First, we have:

Definition 1 (Measurements and State Variables in Gas Systems): This paper defines \mathbf{z}^g and \mathbf{x}^g as the vectors of measurements and state variables in a gas system, respectively. $\mathbf{z}^g = \text{col}(g_i, g_{ij}, c_{mn}, \pi_i), i \in \mathcal{G}_n, \{i, j\} \in \mathcal{G}_l, \{m, n\} \in \mathcal{G}_c$, i.e., gas injections, gas flows in gas passive pipelines, gas flows in gas compressors, and nodal pressures. $\mathbf{x}^g = \text{col}(c_{ij}, \pi_i), \{i, j\} \in \mathcal{G}_c, i \in \mathcal{G}_n$, i.e., gas flows in gas compressors and nodal pressures.

Gas system measurements and state variables satisfy

$$\mathbf{z}^g = \mathbf{h}^g(\mathbf{x}^g) + \mathbf{e}^g, \quad (6)$$

where $\mathbf{h}^g(\cdot)$ is the vector of functions that maps gas system state variables into corresponding measurements. Please refer to (B.5)-(B.6) in the Appendix for detailed formulations of the nontrivial part of $\mathbf{h}^g(\cdot)$. (The trivial part of $\mathbf{h}^g(\cdot)$ is the identity mappings of c_{ij} and $\pi_i, \{i, j\} \in \mathcal{G}_c, i \in \mathcal{G}_n$.) $\mathbf{e}^g \sim \mathcal{N}(0, \mathbf{E}^g)$ is the vector of measurement errors. With measurements \mathbf{z}^g , gas system states are estimated by

$$\hat{\mathbf{x}}^g = \arg \min_{\mathbf{x}^g} (\mathbf{z}^g - \mathbf{h}^g(\mathbf{x}^g))^\top \cdot (\mathbf{E}^g)^{-1} \cdot (\mathbf{z}^g - \mathbf{h}^g(\mathbf{x}^g)), \quad (7)$$

where $\hat{\mathbf{x}}^g$ is the vector of estimated gas system states. This work assumes that gas systems are observable [9]-[12], [26].

Remark 1: The state variables \mathbf{x}^g uniquely determine the values of all variables in a gas system. Unlike [26], this paper does not define the gas flows in gas passive pipelines, i.e., $g_{ij}, \{i, j\} \in \mathcal{G}_l$, as state variables. This is due to the fact that the values of g_{ij} can be determined by state variables $\pi_i, i \in \mathcal{G}_n$ (via (B.5) in the Appendix). Thus, this paper adopts Definition 1 and gas system state estimation (7) as the basis for the following analysis. Note that the gas system state estimation paradigm is not fixed and may vary with practical requirements (e.g., by setting different state variables and measurements).

C. IEGS SE and BDD

Based on the above definition, we develop the static SE of IEGSs. The main difference between the SE of IEGSs and pure power/gas systems is that the former considers power-gas interdependency (e.g., gas supply to gas-fired power generators). The next section shows how the interdependency affects FDIAs on IEGSs. First, we give the following definition.

Definition 2 (Measurements and State Variables in IEGSs): This paper defines \mathbf{z} and \mathbf{x} as the vectors of measurements and state variables in an IEGS, respectively, where $\mathbf{z} = \text{col}(\mathbf{z}^p, \mathbf{z}^g)$ and $\mathbf{x} = \text{col}(\mathbf{x}^p, \mathbf{x}^g)$.

Measurements and state variables in an IEGS satisfy

$$\mathbf{z} = \mathbf{h}(\mathbf{x}) + \mathbf{e}, \quad (8)$$

where $\mathbf{h}(\cdot) = \text{col}(\mathbf{h}^p(\cdot), \mathbf{h}^g(\cdot))$, and $\mathbf{e} \sim \mathcal{N}(0, \mathbf{E})$ is the vector of measurement errors. In view of the interdependency between power and gas systems in an IEGS, e.g., the gas supply to gas-fired power generators, (see (B.9) and (B.10) in the Appendix for details.) the estimated IEGS states $\hat{\mathbf{x}}$ are derived by

$$\hat{\mathbf{x}} = \arg \min_{\mathbf{x}} (\mathbf{z} - \mathbf{h}(\mathbf{x}))^\top \cdot \mathbf{E}^{-1} \cdot (\mathbf{z} - \mathbf{h}(\mathbf{x})) \quad (9a)$$

$$\text{s.t. } \mathbf{T} \cdot \mathbf{h}_c^p(\mathbf{x}^p) = \mathbf{h}_c^g(\mathbf{x}^g), \quad (9b)$$

where constraint (9b) is the vector form of (B.10). \mathbf{T} is a diagonal matrix, whose diagonal elements are $\gamma_g, g \in \mathcal{G}_g$.

Remark 2: Physically, the outputs of gas-fired power gener-

ators that satisfy assumptions A.i)-A.iii) (in the Appendix) can be estimated by either power system state variables \mathbf{x}^p , i.e., $\mathbf{h}_c^p(\mathbf{x}^p)$ via (B.1), (B.3), and (B.7), or gas system state variables \mathbf{x}^g , i.e., $\mathbf{T}^{-1} \cdot \mathbf{h}_c^g(\mathbf{x}^g)$ via (B.5), (B.6), and (B.9). Constraint (9b) ensures that the estimated outputs of gas-fired power generators are consistent. Specifically, constraint (9b) ensures the consistency between $\mathbf{T} \cdot \mathbf{h}_c^p(\mathbf{x}^p)$ and $\mathbf{h}_c^g(\mathbf{x}^g)$, which is different from auxiliary constraints aiming at enhancing the accuracy of SE, e.g., zero injection constraints [27], and is indispensable for IEGS SE. An illustrative case is presented in Section V.A 1) to validate the importance of (9b), a. Since we assume that IEGSs are observable, model (9) can determine all state variables \mathbf{x} by measurements \mathbf{z} . This assumption is based on the fact that both power and gas systems have sufficient meters for measurement collection [6]- [22], [26], yielding observable IEGSs.

In order to check if there are bad data in IEGS measurements \mathbf{z} during the above SE, we develop the following BDD:

$$\|\mathbf{r}\| = \|\mathbf{z} - \mathbf{h}(\hat{\mathbf{x}})\| \leq \tau, \quad (10a)$$

$$\|\mathbf{r}_c\| = \|\mathbf{T} \cdot \mathbf{h}_c^p(\hat{\mathbf{x}}^p) - \mathbf{h}_c^g(\hat{\mathbf{x}}^g)\| \leq \epsilon. \quad (10b)$$

\mathbf{r} and \mathbf{r}_c are the vectors of residuals for all IEGS measurements and coupling measurements, respectively. Coupling measurements refer to gas-fired generator output measurements. If $\|\mathbf{r}\|$ is larger than τ , a threshold, or $\|\mathbf{r}_c\|$ is larger than ϵ , a small positive number, e.g., $1e-5$ (from numerical consideration), bad data exist in measurements \mathbf{z} . Constraint (10a) is similar to the BDD in power systems, while constraint (10b) is specifically designed for IEGS BDD to avoid inconsistent estimation and detect the FDIAs that ignore coupling constraint (9b).

III. FDIAs ON IEGSs WITH COMPLETE NETWORK INFORMATION

In this section, we propose (stealthy) FDIAs on IEGSs with complete network information.

A. The Proposed FDIAs on IEGSs

This subsection proposes (stealthy) FDIAs on IEGS SE (9). Note that existing FDIAs on pure power systems [6]-[8] do not consider coupling constraints (9b) in IEGSs (i.e., CAI) and are detectable by (10) if directly adopted to compromise an IEGS. Differently, the proposed FDIAs consider (9b) and thus can bypass (10). Before proceeding, we assume that i) true measurements \mathbf{z} can pass IEGS BDD, ii) intruders have full knowledge of network information $\mathbf{h}(\cdot)$, iii) intruders can get access to all measurements \mathbf{z} , and iv) intruders have the same estimated states $\hat{\mathbf{x}}$ as those estimated by IEGS operators [7], [19].

Then, we present the proposed FDIAs on IEGSs. Let $\Delta\mathbf{z} = \text{col}(\Delta\mathbf{z}^p, \Delta\mathbf{z}^g)$ be the vector of injected false data into measurements \mathbf{z} and $\Delta\mathbf{x} = \text{col}(\Delta\mathbf{x}^p, \Delta\mathbf{x}^g)$ be the vector of variations in estimated states $\hat{\mathbf{x}}$ after the attack. $\Delta\mathbf{z}^g = \text{col}(\Delta g_i, \Delta g_{ij}, \Delta c_{mn}, \Delta\pi_i)$, $i \in \mathcal{G}_n$, $\{i, j\} \in \mathcal{G}_l$, $\{m, n\} \in \mathcal{G}_c$, is the vector of injected false data into measurements \mathbf{z}^g . $\Delta\mathbf{x}^g = \text{col}(\Delta c_{ij}, \Delta\pi_i)$, $\{i, j\} \in \mathcal{G}_c$, $i \in \mathcal{G}_n$, is the vector of variations in estimated states $\hat{\mathbf{x}}^g$ after the attack. (The definitions of $\Delta\mathbf{z}^p$ and $\Delta\mathbf{x}^p$ are given in Section II.A.) If an attack $\Delta\mathbf{z}$ satisfies

$$\Delta\mathbf{z} = \mathbf{h}(\hat{\mathbf{x}} + \Delta\mathbf{x}) - \mathbf{h}(\hat{\mathbf{x}}), \quad (11a)$$

$$\|\mathbf{T} \cdot \mathbf{h}_c^p(\hat{\mathbf{x}}^p + \Delta\mathbf{x}^p) - \mathbf{h}_c^g(\hat{\mathbf{x}}^g + \Delta\mathbf{x}^g)\| \leq \epsilon, \quad (11b)$$

this attack $\Delta\mathbf{z}$ is an FDIA and can compromise an IEGS without being detected by IEGS BDD (10).

We check if the above FDIA $\Delta\mathbf{z}$ can bypass IEGS BDD (10). Let $\mathbf{z}_{\text{bad}} = \mathbf{z} + \Delta\mathbf{z}$ and $\mathbf{x}_{\text{bad}} = \hat{\mathbf{x}} + \Delta\mathbf{x}$. \mathbf{z}_{bad} and \mathbf{x}_{bad} are vectors of falsified measurements and estimated states under falsified measurements \mathbf{z}_{bad} , respectively. For \mathbf{z}_{bad} , the residuals become

$$\begin{aligned} \|\mathbf{r}_{\text{bad}}\| &= \|\mathbf{z}_{\text{bad}} - \mathbf{h}(\mathbf{x}_{\text{bad}})\| \\ &= \|\mathbf{z} + \Delta\mathbf{z} - \mathbf{h}(\hat{\mathbf{x}} + \Delta\mathbf{x})\| \\ &= \|\mathbf{z} + \mathbf{h}(\hat{\mathbf{x}} + \Delta\mathbf{x}) - \mathbf{h}(\hat{\mathbf{x}}) - \mathbf{h}(\hat{\mathbf{x}} + \Delta\mathbf{x})\| \\ &= \|\mathbf{z} - \mathbf{h}(\hat{\mathbf{x}})\| = \|\mathbf{r}\| \leq \tau, \end{aligned} \quad (12a)$$

$$\begin{aligned} \|\mathbf{r}_{c, \text{bad}}\| &= \|\mathbf{T} \cdot \mathbf{h}_c^p(\mathbf{x}_{\text{bad}}^p) - \mathbf{h}_c^g(\mathbf{x}_{\text{bad}}^g)\| \\ &= \|\mathbf{T} \cdot \mathbf{h}_c^p(\hat{\mathbf{x}}^p + \Delta\mathbf{x}^p) - \mathbf{h}_c^g(\hat{\mathbf{x}}^g + \Delta\mathbf{x}^g)\| \leq \epsilon, \end{aligned} \quad (12b)$$

where \mathbf{r}_{bad} and $\mathbf{r}_{c, \text{bad}}$ are the vectors of residuals for all falsified IEGS measurements and coupling measurements, respectively. $\mathbf{x}_{\text{bad}}^g = \hat{\mathbf{x}}^g + \Delta\mathbf{x}^g$. Since conditions (10) hold, the designed FDIA $\Delta\mathbf{z}$ can bypass IEGS BDD.

Remark 3: Conditions (11) keep the residuals of BDD (before and after FDIAs on IEGSs) the same. Particularly, condition (11b) is designed to ensure that coupling constraint (9b) holds, which is crucial and also the main difference between the proposed FDIAs on IEGSs and those on pure power systems [6]-[8]. We will show in Section V.A 2) that the FDIAs on pure power systems cannot be applied to compromise the power subsystem in an IEGS due to the violation of condition (11b).

The above analysis is based on the assumption that intruders have the same estimated states as those estimated by IEGS operators. In fact, this may not always be true [28]. Please refer to [29] for the analysis when this assumption does not hold.

B. Extension

The proposed FDIAs on IEGSs in Section III.A are versatile and can cover the following cases by simple extensions.

1) *Constraint violation.* Although conditions (11) ensure the stealthiness of FDIAs on IEGSs, i.e., (12) holds, these FDIAs may still cause constraint violation and arouse suspicion. To avoid FDIA-induced constraint violation, intruders should consider both conditions (11) and the following constraints.

$$\sqrt{(\hat{p}_{ij} + \Delta p_{ij})^2 + (\hat{q}_{ij} + \Delta q_{ij})^2} \leq S_{ij}^{\max}, \quad \forall \{i, j\} \in \mathcal{P}_l, \quad (13a)$$

$$V_i^{\min} \leq \hat{v}_i + \Delta v_i \leq V_i^{\max}, \quad \forall i \in \mathcal{P}_n, \quad (13b)$$

$$-\theta_i^{\max} \leq \hat{\theta}_i + \Delta\theta_i \leq \theta_i^{\max}, \quad \forall i \in \mathcal{P}_n, \quad (13c)$$

$$P_i^{\min} \leq \hat{p}_i + \Delta p_i \leq P_i^{\max}, \quad \forall i \in \mathcal{P}_n, \quad (13d)$$

$$Q_i^{\min} \leq \hat{q}_i + \Delta q_i \leq Q_i^{\max}, \quad \forall i \in \mathcal{P}_n, \quad (13e)$$

$$-G_{ij}^{\max} \leq \hat{g}_{ij} + \Delta g_{ij} \leq G_{ij}^{\max}, \quad \forall \{i, j\} \in \mathcal{G}_l, \quad (13f)$$

$$0 \leq \hat{c}_{ij} + \Delta c_{ij} \leq C_{ij}^{\max}, \quad \forall \{i, j\} \in \mathcal{G}_c, \quad (13g)$$

$$\Pi_i^{\min} \leq \hat{\pi}_i + \Delta\pi_i \leq \Pi_i^{\max}, \quad \forall i \in \mathcal{G}_n, \quad (13h)$$

$$\hat{\pi}_j + \Delta\pi_j \leq \alpha_{ij}(\hat{\pi}_i + \Delta\pi_i), \quad \forall \{i, j\} \in \mathcal{G}_c, \quad (13i)$$

$$G_i^{\min} \leq \hat{g}_i + \Delta g_i \leq G_i^{\max}, \quad \forall i \in \mathcal{G}_n, \quad (13j)$$

where \hat{p}_{ij} , \hat{q}_{ij} , \hat{g}_{ij} , \hat{p}_i , \hat{q}_i , \hat{g}_i are the elements of $\mathbf{h}(\hat{\mathbf{x}})$, i.e., estimated measurements, and \hat{v}_i , $\hat{\theta}_i$, \hat{c}_{ij} , $\hat{\pi}_i$ are the elements of $\hat{\mathbf{x}}$, i.e., estimated states. Constraints (13a)-(13e) are the thermal limit, voltage magnitude boundary, phase angle range, and real and reactive power injection limitation, respectively. Particularly, by setting the corresponding bounds, constraints (13d) and (13e) can be used to guarantee that: i) the falsified power in-

jection measurements at zero power injection buses are zero, ii) the falsified power injection measurements at the power buses that are connected with only power loads are no larger than zero, and iii) the falsified power injection measurements at the power buses that are connected with only power generators are within generator output capacities. Constraints (13f)-(13j) specify the transmission capability of gas passive pipelines and gas compressors, nodal pressure boundary, gas compressor limit, and gas injection limitation, respectively. Similar to (13d) and (13e), constraint (13j) regulates gas injections at gas nodes.

2) *Compressor model.* Section III.A uses a simplified gas compressor model [30], which applies to large-scale gas networks with compressor stations [25]. For small- and medium-scale IEGSSs, the simplified model may not be accurate enough. See [29] for FDIAs on IEGSSs with detailed compressor models.

3) *Power-to-gas (P2G) facility.* IEGSSs may include P2G facilities [31]. These can transform (surplus) electricity into natural gas. Similar to gas-fired generators, P2G facilities introduce coupling relations to IEGSSs. Please refer to [29] for accurate state estimation of P2G facility-embedded IEGSSs.

IV. FDIAs ON IEGSSS WITH INCOMPLETE NETWORK INFORMATION

This section relaxes the strong assumption adopted in Section III, which requires intruders have complete network (topology and parameter) information, and develops FDIAs on IEGSSs with incomplete network information (to be precise, with local network (topology and parameter) information (Section IV.A) and local topology information (Section IV.B)).

A. FDIAs on IEGSSs With Local Network Information

Without loss of generality, this subsection divides a connected IEGSS into two regions, i.e., an attacking region and a non-attacking region. Intruders are assumed to have i) complete/zero network information of the attacking/non-attacking region, and ii) all/zero measurement in the attacking/non-attacking region. The attacking region may consist of several areas in an IEGSS without (direct) connectivity requirement (between these areas). So does the non-attacking region. The direct connectivity between two areas means that there exists at least one tie line or at least one gas-fired generator that physically connects these two areas. Fig. 1 shows an example. The attacking/non-attacking region consists of A1/N1 (an area of the power system part in an IEGSS) and A2/N2 (an area of the gas system part in an IEGSS). Power transmission line $\{i, j\}$, gas passive pipeline $\{m, n\}$, and gas compressor $\{u, v\}$ are tie-lines that connect the attacking region and non-attacking region. Generally, we have

Definition 3 (Boundary nodes): Boundary nodes are defined as i) the power buses and gas nodes that connect to tie-lines in attacking regions, ii) the power buses with gas-fired generators in attacking regions, and iii) the gas nodes that connect to gas-fired generators in attacking regions.

Note that boundary nodes are critical for developing FDIAs on IEGSSs with local network information. Based on Definition 3, in Fig. 1, power bus i and gas nodes m and u are the first type of boundary nodes, and power bus k and gas node o are the second and third types of boundary nodes, respectively.

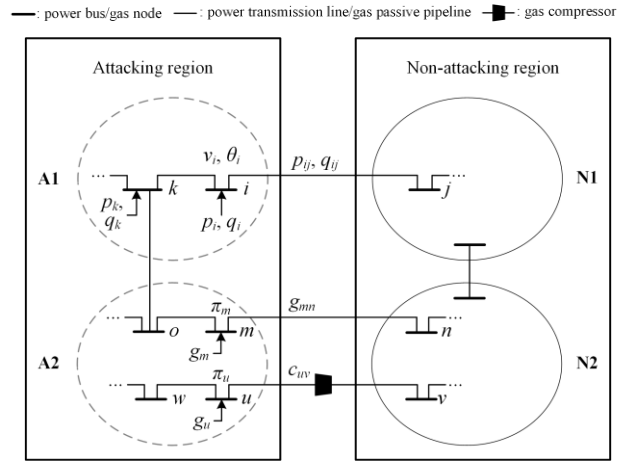


Fig. 1. Illustrative example of attacking and non-attacking regions in an IEGSS.

Let $\mathbf{z} = \text{col}(\mathbf{z}_A, \mathbf{z}_B, \mathbf{z}_N)$ and $\mathbf{x} = \text{col}(\mathbf{x}_A, \mathbf{x}_B, \mathbf{x}_N)$. Vector \mathbf{z}_A is composed of all measurements in the attacking region except for power and gas injection measurements at boundary nodes, vector \mathbf{z}_B contains power and gas injection measurements at boundary nodes, and vector \mathbf{z}_N consists of the rest measurements. Power and gas flow measurements in tie lines between attacking and non-attacking regions, e.g., p_{ij}, q_{ij}, g_{mn} , and c_{uv} in Fig. 1, belong to \mathbf{z}_N . This subsection assumes that the (true) measurements $\mathbf{z} = \text{col}(\mathbf{z}_A, \mathbf{z}_B, \mathbf{z}_N)$ can pass IEGSS BDD. Vector \mathbf{x}_A includes state variables in the attacking region except for state variables at boundary nodes, vector \mathbf{x}_B contains state variables in boundary nodes, and vector \mathbf{x}_N is the rest state variables. Gas flow states in gas compressors, e.g., c_{uv} in Fig. 1, belong to \mathbf{x}_N . Based on this partition, we (equivalently) re-write the correlation between estimated measurements and estimated states, i.e., (8), as follows.

$$\begin{bmatrix} \mathbf{z}_A \\ \mathbf{z}_B \\ \mathbf{z}_N \end{bmatrix} = \begin{bmatrix} \mathbf{h}_A(\mathbf{x}_A, \mathbf{x}_B) \\ \mathbf{h}_B^A(\mathbf{x}_A, \mathbf{x}_B) + \mathbf{h}_B^N(\mathbf{x}_N, \mathbf{x}_B) \\ \mathbf{h}_N(\mathbf{x}_N, \mathbf{x}_B) \end{bmatrix} + \begin{bmatrix} \mathbf{e}_A \\ \mathbf{e}_B \\ \mathbf{e}_N \end{bmatrix}, \quad (14)$$

where $\mathbf{h}_A(\cdot)$, $\mathbf{h}_B^A(\cdot)$, $\mathbf{h}_B^N(\cdot)$, $\mathbf{h}_N(\cdot)$, \mathbf{e}_A , \mathbf{e}_B , and \mathbf{e}_N are determined accordingly. Tie line information belongs to $\mathbf{h}_N(\cdot)$. Since intruders know the measurements and network information of the attacking region, in (14), they know: i) measurements \mathbf{z}_A and \mathbf{z}_B , and ii) network information $\mathbf{h}_A(\cdot)$ and $\mathbf{h}_B^A(\cdot)$, and they do not know i) \mathbf{z}_N , or ii) $\mathbf{h}_B^N(\cdot)$ or $\mathbf{h}_N(\cdot)$.

Then, we introduce the proposed FDIAs on IEGSSs with local network information. Let $\Delta\mathbf{z}_A$, $\Delta\mathbf{z}_B$, and $\Delta\mathbf{z}_N$ be the vectors of injected false data into measurements \mathbf{z}_A , \mathbf{z}_B , and \mathbf{z}_N , respectively, and let $\Delta\mathbf{x}_A$, $\Delta\mathbf{x}_B$, and $\Delta\mathbf{x}_N$ be the variations in estimated states $\hat{\mathbf{x}}_A$, $\hat{\mathbf{x}}_B$, and $\hat{\mathbf{x}}_N$, respectively, after the attack. If an attack $\Delta\mathbf{z} = \text{col}(\Delta\mathbf{z}_A, \Delta\mathbf{z}_B, \Delta\mathbf{z}_N)$ satisfies

$$\Delta\mathbf{z}_A = \mathbf{h}_A(\hat{\mathbf{x}}_A + \Delta\mathbf{x}_A, \hat{\mathbf{x}}_B) - \mathbf{h}_A(\hat{\mathbf{x}}_A, \hat{\mathbf{x}}_B) \quad (15a)$$

$$\Delta\mathbf{z}_B = \mathbf{h}_B^A(\hat{\mathbf{x}}_A + \Delta\mathbf{x}_A, \hat{\mathbf{x}}_B) - \mathbf{h}_B^A(\hat{\mathbf{x}}_A, \hat{\mathbf{x}}_B) \quad (15b)$$

$$\Delta\mathbf{z}_N = \mathbf{0}, \quad (15c)$$

where $\Delta\mathbf{x}_A$ can be any real vector, this attack $\Delta\mathbf{z}$ is a (stealthy) FDIA, which can compromise an IEGSS without being detected by IEGSS BDD (10). Note that conditions (15) implicitly require that $\Delta\mathbf{x}_B$ and $\Delta\mathbf{x}_N$ are both zero vectors.

To show that, we first check (10a). For falsified measurements $\mathbf{z} + \Delta\mathbf{z}$, IEGSS BDD (10a) becomes

$$\begin{aligned}
\|\mathbf{r}_{\text{bad}}\| &= \left\| \begin{bmatrix} \mathbf{z}_A + \Delta\mathbf{z}_A - \mathbf{h}_A(\hat{\mathbf{x}}_A + \Delta\mathbf{x}_A, \hat{\mathbf{x}}_B) \\ \mathbf{z}_B + \Delta\mathbf{z}_B - (\mathbf{h}_B^A(\hat{\mathbf{x}}_A + \Delta\mathbf{x}_A, \hat{\mathbf{x}}_B) + \mathbf{h}_B^N(\hat{\mathbf{x}}_N, \hat{\mathbf{x}}_B)) \\ \mathbf{z}_N + \Delta\mathbf{z}_N - \mathbf{h}_N(\hat{\mathbf{x}}_N, \hat{\mathbf{x}}_B) \end{bmatrix} \right\| \\
&= \left\| \begin{bmatrix} \mathbf{z}_A + \mathbf{h}_A(\hat{\mathbf{x}}_A + \Delta\mathbf{x}_A, \hat{\mathbf{x}}_B) - \mathbf{h}_A(\hat{\mathbf{x}}_A, \hat{\mathbf{x}}_B) - \\ \mathbf{z}_B + \mathbf{h}_B^A(\hat{\mathbf{x}}_A + \Delta\mathbf{x}_A, \hat{\mathbf{x}}_B) - \mathbf{h}_B^A(\hat{\mathbf{x}}_A, \hat{\mathbf{x}}_B) - \\ \mathbf{z}_N + \mathbf{0} - \\ \mathbf{h}_A(\hat{\mathbf{x}}_A + \Delta\mathbf{x}_A, \hat{\mathbf{x}}_B) \\ (\mathbf{h}_B^A(\hat{\mathbf{x}}_A + \Delta\mathbf{x}_A, \hat{\mathbf{x}}_B) + \mathbf{h}_B^N(\hat{\mathbf{x}}_N, \hat{\mathbf{x}}_B)) \\ \mathbf{h}_N(\hat{\mathbf{x}}_N, \hat{\mathbf{x}}_B) \end{bmatrix} \right\| \\
&= \left\| \begin{bmatrix} \mathbf{z}_A - \mathbf{h}_A(\hat{\mathbf{x}}_A, \hat{\mathbf{x}}_B) \\ \mathbf{z}_B - (\mathbf{h}_B^A(\hat{\mathbf{x}}_A, \hat{\mathbf{x}}_B) + \mathbf{h}_B^N(\hat{\mathbf{x}}_N, \hat{\mathbf{x}}_B)) \\ \mathbf{z}_N - \mathbf{h}_N(\hat{\mathbf{x}}_N, \hat{\mathbf{x}}_B) \end{bmatrix} \right\| = \|\mathbf{r}\| \leq \tau,
\end{aligned}$$

The equation in the last row is derived from (15), indicating that the FDIA $\Delta\mathbf{z}$ can bypass (10a). Then, we check if this FDIA can be detected by IEGS BDD (10b). According to Definition 3, the power buses and gas nodes connected to gas-fired generators in an attacking region are boundary nodes. According to (15), the FDIA $\Delta\mathbf{z}$ does not change the states of boundary nodes. So, the FDIA $\Delta\mathbf{z}$ cannot be detected by (10b). Overall, we conclude that the FDIA $\Delta\mathbf{z}$ cannot be detected by IEGS BDD (10).

Remark 4: To guarantee the stealthiness of an FDIA, injected false data $\Delta\mathbf{z}$ can be derived by setting $\Delta\mathbf{x}_B = \mathbf{0}$ and $\Delta\mathbf{x}_N = \mathbf{0}$. For the variation of estimated states $\hat{\mathbf{x}}_A$, i.e., $\Delta\mathbf{x}_A$, theoretically, it can be any vector. In practice, it can be designed by considering the constraints in Section III.B to enhance stealthiness.

Based on the above analysis, we immediately derive

Corollary 1: Intruders can launch a (stealthy) FDIA $\Delta\mathbf{z}$ on an IEGS with local network (topology and parameter) information (i.e., $\mathbf{h}_A(\cdot)$ and $\mathbf{h}_B^A(\cdot)$) if i) they know local estimated states (i.e., $\hat{\mathbf{x}}_A$ and $\hat{\mathbf{x}}_B$), and ii) conditions (15) are satisfied.

According to Corollary 1, the proposed (stealthy) FDIAs require that intruders should have accurate estimated states in the attacking region (i.e., $\hat{\mathbf{x}}_A$ and $\hat{\mathbf{x}}_B$). Accurate estimated states are the states estimated by IEGS operators with true measurements \mathbf{z} , which is elusive. For this case, intruders can estimate the states in the attacking region (denoted as $\hat{\mathbf{x}}'_A$ and $\hat{\mathbf{x}}'_B$) based on measurements \mathbf{z}_A and \mathbf{z}'_B . We take the IEGS in Fig. 1 as an example for clarifying how to generate \mathbf{z}'_B and derive estimated states. Let $p'_i = p_i - p_{ij}$, $q'_i = q_i - q_{ij}$, $g'_m = g_m - g_{mn}$, and $g'_u = g_u - c_{uv}$. Measurements p'_i, q'_i, g'_m , and g'_u are revised power and gas injection measurements at boundary nodes. $\mathbf{z}'_B = \text{col}(p'_i, q'_i, g'_m, g'_u)$. Intruders can utilize \mathbf{z}_A and \mathbf{z}'_B to conduct SE (in the attacking region) and derive $\hat{\mathbf{x}}'_A$ and $\hat{\mathbf{x}}'_B$. Due to the existence of biases between $\hat{\mathbf{x}}_A, \hat{\mathbf{x}}_B$ and $\hat{\mathbf{x}}'_A, \hat{\mathbf{x}}'_B$, intruders may consider analyzing the impact of biases on the stealthiness of any FDIAs by using the method proposed in Section III.A. In addition, intruders can determine their target area in an attacking region by following the method proposed in [32]. Note that the model extensions (in Section III.B) are also applicable to extending the FDIAs presented in this subsection.

B. FDIAs on IEGSs With Only Local Topology Information

This subsection further relaxes the assumption in Section

IV.A, which requires intruders have local network (topology and parameter) information. Specifically, in this subsection, intruders are assumed to have: i) complete topology information of the attacking region, ii) zero parameter information of the attacking region, iii) zero network (topology and parameter) information of the non-attacking region, iv) all measurements in the attacking region, and v) zero measurements in the non-attacking region. In addition, this subsection assumes (true) measurements \mathbf{z} can pass IEGS BDD. Accordingly, we have the following Lemma:

Lemma 1: If intruders only have local topology information of an IEGS, the stealthiness of injected false data on any *power system measurements* in this IEGS cannot be guaranteed.

Proof: We start with a *Simple Case*, where intruders have topology information of an entire IEGS, i.e., the attacking region is the entire IEGS. Let constant matrices \mathbf{B}^p and \mathbf{B}^g be the incidence matrices of power and gas systems in an IEGS, respectively. Specifically, matrix $\mathbf{B}^p/\mathbf{B}^g$ has one row for each power bus/gas node and one column for each power transmission line/gas pipeline (either a gas passive pipeline or a gas compressor). The element in row i and column j in $\mathbf{B}^p/\mathbf{B}^g$ is i) 1 if power transmission line/gas pipeline j is connected to power bus/gas node i with power/gas *outflow* to i , ii) -1 if power transmission line/ gas pipeline j is connected to power bus/gas node i with power/ gas *inflow* to i , and iii) 0 if they are not connected. Let vector $\mathbf{p}_{ij} = \text{col}(p_{ij})$, $\{i, j\} \in \mathcal{P}_l$. Similarly, we derive vectors $\mathbf{q}_{ij}, \mathbf{p}_j, \mathbf{q}_j, \mathbf{v}_j, \boldsymbol{\theta}_{l'}, \mathbf{g}_{lj}, \mathbf{g}_j, \boldsymbol{\pi}_j$, and \mathbf{c}_{lj} . Detailed (mathematical) correlation between estimated measurements (i.e., $\hat{\mathbf{p}}_{lj}, \hat{\mathbf{q}}_{lj}, \hat{\mathbf{p}}_j, \hat{\mathbf{q}}_j, \hat{\mathbf{v}}_j, \hat{\boldsymbol{\theta}}_{l'}, \hat{\mathbf{g}}_{lj}, \hat{\mathbf{g}}_j, \hat{\boldsymbol{\pi}}_j, \hat{\mathbf{c}}_{lj}$) and estimated states (i.e., $\hat{\mathbf{v}}_j, \hat{\boldsymbol{\theta}}_j, \hat{\boldsymbol{\pi}}_j, \hat{\mathbf{c}}_{lj}$) are shown as follows:

$$\mathbf{h}^p(\hat{\mathbf{x}}^p) = \begin{bmatrix} [\hat{\mathbf{p}}_{lj}^T, \hat{\mathbf{q}}_{lj}^T]^T \\ [\hat{\mathbf{p}}_j^T, \hat{\mathbf{q}}_j^T]^T \\ [\hat{\mathbf{v}}_j^T, \hat{\boldsymbol{\theta}}_{l'}^T]^T \end{bmatrix} = \begin{bmatrix} \mathbf{h}_1^p([\hat{\mathbf{v}}_j^T, \hat{\boldsymbol{\theta}}_{l'}^T]^T) \\ \mathbf{h}_2^p([\hat{\mathbf{v}}_j^T, \hat{\boldsymbol{\theta}}_{l'}^T]^T) \\ \mathbf{h}_3^p([\hat{\mathbf{v}}_j^T, \hat{\boldsymbol{\theta}}_{l'}^T]^T) \end{bmatrix} = \begin{bmatrix} \mathbf{h}_1^p([\hat{\mathbf{v}}_j^T, \hat{\boldsymbol{\theta}}_{l'}^T]^T) \\ \mathbf{D} \cdot \mathbf{h}_1^p([\hat{\mathbf{v}}_j^T, \hat{\boldsymbol{\theta}}_{l'}^T]^T) \\ \mathbf{I}^p \cdot [\hat{\mathbf{v}}_j^T, \hat{\boldsymbol{\theta}}_{l'}^T]^T \end{bmatrix}, \quad (16a)$$

$$\mathbf{h}^g(\hat{\mathbf{x}}^g) = \begin{bmatrix} \hat{\mathbf{g}}_{lj} \\ \hat{\mathbf{g}}_j \\ [\hat{\boldsymbol{\pi}}_j^T, \hat{\mathbf{c}}_{lj}^T]^T \end{bmatrix} = \begin{bmatrix} \mathbf{h}_1^g(\hat{\boldsymbol{\pi}}_j) \\ \mathbf{h}_2^g([\hat{\boldsymbol{\pi}}_j^T, \hat{\mathbf{c}}_{lj}^T]^T) \\ \mathbf{h}_3^g([\hat{\boldsymbol{\pi}}_j^T, \hat{\mathbf{c}}_{lj}^T]^T) \end{bmatrix} = \begin{bmatrix} \mathbf{h}_1^g(\hat{\boldsymbol{\pi}}) \\ \mathbf{B}_h^g \cdot \mathbf{h}_1^g(\hat{\boldsymbol{\pi}}) + \mathbf{B}_c^g \cdot \hat{\mathbf{c}}_{lj} \\ \mathbf{I}^g \cdot [\hat{\boldsymbol{\pi}}_j^T, \hat{\mathbf{c}}_{lj}^T]^T \end{bmatrix}, \quad (16b)$$

$$\begin{aligned}
\mathbf{T} \cdot \mathbf{h}_c^p(\hat{\mathbf{x}}^p) &= \mathbf{T}^p \cdot \mathbf{D}' \cdot \mathbf{h}_1^p([\hat{\mathbf{v}}_j^T, \hat{\boldsymbol{\theta}}_{l'}^T]^T) \\
&= \mathbf{h}_c^g(\hat{\mathbf{x}}^g) = \mathbf{T}^g \cdot \mathbf{B}^g \cdot [\mathbf{h}_1^g(\hat{\boldsymbol{\pi}})^T, \hat{\mathbf{c}}_{lj}^T]^T. \quad (16c)
\end{aligned}$$

$\mathbf{h}_1^p(\cdot), \mathbf{h}_2^p(\cdot), \mathbf{h}_3^p(\cdot)$, and $\mathbf{h}_2^g(\cdot)$ refer to the mappings (B.1)-(B.2), (B.3)-(B.4), (B.5), and (B.6), respectively, in the Appendix. $\mathbf{h}_3^p(\cdot)$ and $\mathbf{h}_3^g(\cdot)$ denote mappings \mathbf{I}^p and \mathbf{I}^g , respectively. \mathbf{I}^g is an identity matrix, and $\mathbf{I}^p, \mathbf{T}^p$ and \mathbf{T}^g are constant matrices. $\mathbf{B}^g = [\mathbf{B}_h^g \ \mathbf{B}_c^g]$. Constant matrices

$$\mathbf{D} = \begin{bmatrix} \mathbf{B}^p & \mathbf{M}_0 \\ \mathbf{M}_0^T & \mathbf{B}^p \end{bmatrix}, \quad \mathbf{D}' = \begin{bmatrix} \mathbf{B}^p & \mathbf{M}_0 \\ \mathbf{M}_0^T & \mathbf{N}_0 \end{bmatrix},$$

where \mathbf{M}_0 and \mathbf{N}_0 are all-zero matrices. Mathematically, the Simple Case means that intruders know matrices $\mathbf{D}, \mathbf{D}', \mathbf{I}^p, \mathbf{T}^p, \mathbf{B}_h^g, \mathbf{B}_c^g, \mathbf{I}^g$, and \mathbf{T}^g but do not know $\mathbf{h}_1^p(\cdot), \mathbf{h}_2^p(\cdot), \mathbf{h}_c^p(\cdot), \mathbf{h}_1^g(\cdot), \mathbf{h}_2^g(\cdot), \mathbf{h}_c^g(\cdot)$, or \mathbf{T} , as intruders have no parameter information.

If intruders have the topology information of an entire IEGS and launch an FDIA on *power system measurements*, according

to (16a), except for Special FDIA 1¹, the stealthiness of any FDIA cannot be guaranteed. This is due to the fact that intruders cannot precisely quantify the injected false data without parameter information (i.e., $\mathbf{h}_1^p(\cdot)$ and $\mathbf{h}_2^p(\cdot)$ in (16a)). Thus, the FDIA has a high possibility of incurring inconsistency between falsified measurements, which are detectable by BDD. For the general case where intruders have *local* topology information of an IEGS, the stealthiness of Special FDIA 1 cannot be guaranteed, either. This is because intruders cannot inject false data into the phase angle measurements in the non-attacking region (according to its definition), where PMUs may be installed. This completes the proof. ■

Lemma 1 indicates that with only local topology information, intruders should not launch FDIAs on any power system measurements in an IEGS. Counter intuitively, we find that the intruders may launch stealthy FDIAs on gas system measurements with only local topology information.

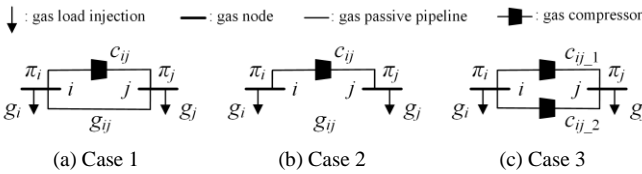


Fig. 2. Illustrative FDIAs on an IEGS with only network topology information.

Lemma 2: If i) intruders only have local topology information of an IEGS, and ii) this local region has nonzero gas load nodes that are connected by at least one gas compressor, intruders can launch (stealthy) FDIAs on this IEGS.

Proof: Let us continue with the Simple Case (presented in the proof of Lemma 1), where intruders have topology information of an *entire* IEGS and launch an FDIA on *gas system measurements* in the IEGS. The second row of (16b) explicitly show \mathbf{g}_j has an affine relation with \mathbf{c}_{ij} . Particularly, intruders know the affine relation exactly, as they know \mathbf{B}_h^g and \mathbf{B}_c^g . Theoretically, intruders are able to launch stealthy FDIAs on gas system measurements \mathbf{g}_j and \mathbf{c}_{ij} .

Mathematically, if intruders manage to inject false data Δg_i into gas compressor c_{ij} , where the connected gas nodes i and j are non-zero gas load nodes, intruders can modify gas injection g_i and g_j by $\mathbf{B}_c^g[i, :] \Delta c_{ij}$ and $\mathbf{B}_c^g[j, :] \Delta c_{ij}$, respectively, i.e., adding the same amount to both left and right hand sides of the second row of (16b), so that equation (16b) still holds. Note that $\mathbf{B}_c^g[i, :]$ is the i -th row of matrix \mathbf{B}_c^g . The attack vector $\Delta c_{ij} = \text{col}(0, \dots, 0, \Delta g_i, 0, \dots, 0)$, where the order of Δg_i in Δc_{ij} is the same as the order of \hat{c}_{ij} in $\hat{\mathbf{c}}_{ij}$. Since this attack does not affect other state variables, equations (16a) and (16c) also hold, indicating that this attack is a (stealthy) FDIA. Physically, it means for Case 1 in Fig. 2, where gas nodes i and j are non-zero gas load nodes, attacks $\text{col}(\Delta g_i, -\Delta g_i, \Delta g_i)$ (on measurements $\text{col}(g_i, g_j, c_{ij})$) are (stealthy) FDIAs. In fact, the FDIAs, i.e., $\text{col}(\Delta g_i, -\Delta g_i, \Delta g_i)$ on measurements $\text{col}(g_i, g_j, c_{ij})$, are general

¹ Special FDIA 1 refers to the FDIA where intruders inject the same false data into all phase angle measurements $\theta_{i'}$, $i' \in \mathcal{P}_n'$. Since the values of trigonometric terms in (B.1) and (B.2) (i.e., $\cos(\cdot)$ and $\sin(\cdot)$) remain the same before and after Special FDIA 1, the values of measurements $\mathbf{p}_{L'}$, $\mathbf{q}_{L'}$, $\mathbf{p}_{I'}$, $\mathbf{q}_{I'}$, and $\mathbf{v}_{I'}$ in (16a) remain the same. Thus, Special FDIA 1 is stealthy.

(stealthy) FDIAs, since they are still valid if we remove gas passive pipeline g_{ij} (e.g., Case 2) or add gas passive pipelines and/or gas compressors to Case 2 (e.g., Case 3), enabling Case 1 to cover all scenarios in Lemma 2. This completes the proof. ■

Lemma 2 confirms that there exist stealthy FDIAs on an IEGS even if intruders only have local topology information of the IEGS. According to the above example, these FDIAs redistribute gas loads at gas nodes i and j (via gas compressor c_{ij}) and are called *gas load redistribution attacks*. In addition to Lemma 2, we have another type of stealthy FDIAs on IEGSs with only local topology information. Lemma 3 shows details.

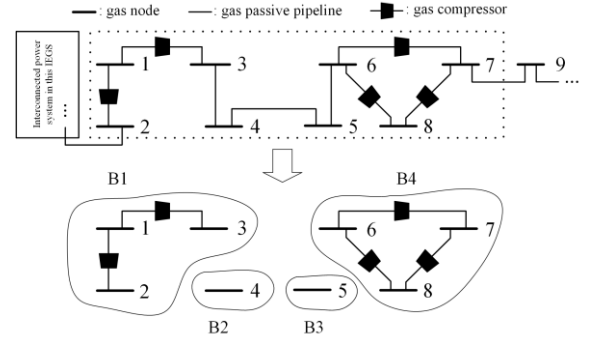


Fig. 3. Illustrative FDIAs on an IEGS with only network topology information of a 8-node gas system containing meshed gas compressors.

Lemma 3: If i) intruders only have local topology information of an IEGS, and ii) this local region has meshed gas compressors, intruders can launch (stealthy) FDIAs on this IEGS.

Proof: Mathematically, if intruders manage to inject false data Δc_{ij} and $-\Delta c_{ij}$ into gas compressor c_{ij_1} and c_{ij_2} , respectively, where c_{ij_1} and c_{ij_2} connect the same gas nodes i and j , we always have $\mathbf{B}_c^g \Delta c_{ij} = \mathbf{0}$, i.e., adding a zero vector to the right hand side of the second row of (16b), so that equation (16b) still holds. The attack vector $\Delta c_{ij} = \text{col}(0, \dots, 0, \Delta c_{ij}, 0, \dots, 0, -\Delta c_{ij}, 0, \dots, 0)$, and the orders of Δc_{ij} and $-\Delta c_{ij}$ in Δc_{ij} are the same as the orders of \hat{c}_{ij_1} and \hat{c}_{ij_2} in $\hat{\mathbf{c}}_{ij}$, respectively. Since this attack does not affect other state variables, equations (16a) and (16c) also hold, indicating that this attack is a (stealthy) FDIA. Physically, it means that for Case 3 in Fig. 2, attacks $\text{col}(\Delta c_{ij}, -\Delta c_{ij})$ (on measurements $\text{col}(c_{ij_1}, c_{ij_2})$) are stealthy FDIAs. In fact, Case 3 can be further generalized as meshed gas compressors, where the gas loads in nodes i and j are not required anymore. Fig. 3 gives an example. Intruders are assumed to have local topology information of an IEGS, i.e., the area within the dotted rectangle in Fig. 3 (an eight-node gas system). To see if this area contains meshed gas compressor, we remove gas passive pipelines and then only consider gas nodes and gas compressors. Consequently, this 8-node gas system is separated into 4 connected subsystems, B1-B4. It is noted that subsystem B4 contains meshed gas compressors. Intruders can launch stealthy FDIAs $\text{col}(\Delta c_{ij}, \Delta c_{ij}, -\Delta c_{ij})$ (on measurements $\text{col}(c_{67}, c_{78}, c_{68})$) on this IEGS. The stealthiness of these FDIAs is similar to the above FDIAs in this proof. In fact, we can always derive stealthy FDIAs on B4 (similar to the general FDIAs $\text{col}(\Delta c_{ij}, \Delta c_{ij}, -\Delta c_{ij})$) if more gas nodes and gas compressors are added (to B4) for generating a larger mesh (i.e., more meshed compressors), enabling B4 to cover all scenarios in Lemma 3.

This completes the proof. \blacksquare

The FDIAs in Lemma 3 redistribute gas flows in gas compressors are called *flow redistribution attacks*. Based on Lemmas 1-3, we immediately derive:

Proposition 1: If i) intruders only have local topology information of an IEGS, and ii) this local region has either meshed gas compressors or non-zero gas load nodes that are connected by at least one gas compressor, intruders can launch (stealthy) FDIAs on this IEGS.

Note that the FDIAs presented in this subsection also applies to the detailed compressor model (introduced in [29]). Before conducting case study, in Table II, we summarize the proposed FDIAs and compare them with the FDIAs in previous works.

TABLE II
SUMMARY OF THE PROPOSED FDIAs AND COMPARISON

Intruders' information	Existence of FDIAs	Conditions of existence	Differences from previous works [6]-[22]
Complete IEGS info. [†]	Yes*	(11)	Considering CAI [†]
Local IEGS (topology and parameter) info.	Yes*	(15)	Not studied before
Local topology info. of an IEGS	No on power subsystem**	NA [†]	Not studied before
	Yes on gas subsystem [‡]	Proposition 1	Not studied before

*: "Yes" denotes there exist (stealthy) FDIAs on IEGSs with the system information indicated in the first column of this table if the conditions in the third column of this table are satisfied.

**": "No on power subsystem" denotes the stealthiness of injected false data on power system measurements in an IEGS with only local topology information of this IEGS cannot be guaranteed.

‡: "Yes for gas subsystem" denotes there exist (stealthy) FDIAs on the gas system in an IEGS even with only local topology information of this IEGS if the conditions in Proposition 1 are satisfied.

†: Info., NA, and CAI are short for information, not applicable, and cyberattack interdependency, resp.

V. CASE STUDY

To validate the effectiveness of FDIAs on IEGSs with complete and incomplete network information, this section conducts tests on an integrated 9-bus-electricity-7-node-gas system (IEGS-9-7) and an integrated 39-bus-electricity-20-node-gas system (IEGS-39-20). Measurements include: i) real and reactive power flows in both ends of power transmission lines, ii) real and reactive power injections at all power buses, iii) voltage magnitudes at all power buses, iv) phase angles at power bus i' , $i' \in \mathcal{P}'_n$, v) gas flows in gas passive pipelines and gas compressors, vi) gas injections at all gas nodes, and vii) nodal pressures at all gas nodes. Measurements are generated by adding random errors (i.e., noise) to optimal energy flow values. IEGS data and measurements are listed in [29]. Tests are coded using Julia 1.6.2 with JuMP on a laptop with an Intel(R) i5-8265U CPU. The solver is Ipopt 3.13.4.

A. Integrated 9-Bus-Electricity-7-Node-Gas System

The IEGS-9-7 contains three generators (coal-fired generator G_1 and gas-fired generators G_2 and G_3), two gas wells (GW_1 and GW_2), three power loads (PL_1 , PL_2 , and PL_3), and three gas loads (GL_1 , GL_2 , and GL_3).

1) *IEGS SE and BDD*. This part shows the importance of coupling constraint (9b) in *IEGS SE and BDD*. Test results are presented in Table III. Scen. is short for scenario. Scen S-A1 and S-A2 denote measurements with low ($2e^{-3}$ variance) and high ($1e^{-2}$ variance) measurement errors, respectively. See [29] for detailed data. O-SE and P-SE denote original SE (9a) and proposed SE (9a)-(9b), respectively. PG and GG are estimated outputs of gas-fired generators by O-SE based on estimated

power system states $\hat{\mathbf{x}}_p$ and estimated gas system states $\hat{\mathbf{x}}_g$, respectively. r_c^O/r_c^P , an element in \mathbf{r}_c (in (10b)), is the residual of one gas-fired generator using the estimated states by O-SE/P-SE. Table III indicates that the estimated outputs by O-SE (i.e., PG and GG) are not consistent, posing IEGS operators a dilemma in deriving bus states. Meanwhile, we observe that inconsistency rises when measurement errors increase (S-A2). Moreover, the estimated outputs of G_2 and G_3 by O-SE of both S-A1 and S-A2 violate IEGS BDD (10b), according to r_c^O . (ϵ in (10b) is set to $1e^{-5}$.) In contrast, the P-SE considers coupling constraint (9b), and the values in r_c^P are zero, indicating the estimated states are trustworthy. This case shows coupling constraint (9b) is indispensable for IEGS SE and BDD.

TABLE III
COMPARISON BETWEEN DIFFERENT STATE ESTIMATION METHODS

Scen.	S-A1 (low noise)				S-A2 (high noise)			
	O-SE	r_c^O	P-SE	r_c^P	O-SE	r_c^O	P-SE	r_c^P
G_2 (MW)	PG: 64.84 GG: 64.88	0.08	64.88	0	PG: 66.89 GG: 65.02	1.87	65.13	0
G_3 (MW)	PG: 10.03 GG: 10.01	0.02	10.01	0	PG: 9.58 GG: 9.48	0.10	9.83	0

2) *FDIAs on IEGSs with complete network information*. This part tests conditions (11) for designing *FDIAs on IEGSs with complete network information* and explains why FDIAs proposed for pure power systems cannot be successfully launched in the power subsystem of an IEGS. Measurement errors are set to be those in Scenario S-A1. Scenarios S-B1, S-B2, and S-B3 denote distinct attack targets, i.e., voltage magnitude v_2 , power and gas injections p_1 and g_6 , and voltage magnitude v_2 (the same as the attack target of S-B1), respectively. Particularly, S-B3 adopts the FDIA paradigms on pure power systems [6]-[8] for compromising the power system in the IEGS without considering the gas subsystem and coupling constraint (9b).

TABLE IV
FDIAs ON IEGSS WITH COMPLETE NETWORK INFORMATION

Scen.	S-B1	S-B2	S-B3
Attack target	v_2	p_1 and g_6	v_2
Affected power state	v_2	$v_2, v_4, v_8, v_9, \theta_1, \theta_2, \theta_4, \theta_5, \theta_7, \theta_8, \theta_9$	v_2
Affected gas state	$c_{42}, \pi_1, \pi_4, \pi_7$	$c_{42}, \pi_1, \pi_2, \pi_4, \pi_6, \pi_7$	-
Residual Before FDIA	$1.2757e^{-2}$	$1.2757e^{-2}$	$1.2757e^{-2}$
Residual After FDIA	$1.2754e^{-2}$	$1.2752e^{-2}$	$10.8227e^{-2}$

Table IV shows that there exist stealthy FDIAs on the IEGS for achieving different attack targets. Specifically, for S-B1, the FDIA (on voltage measurement v_2) induces *fake voltage violation* by changing measurement v_2 from 1.09 p.u. (before the FDIA) to 1.19 p.u. (after the FDIA). (The upper bound is set to 1.1 p.u.) For S-B2, the FDIA (on power injection p_1 and gas injection g_6) incurs *fake uneconomic dispatch*, as this FDIA alters the measurements of the power generator and gas well at power bus 1 and gas node 6. Please refer to [29] for complete test data. Note that although the attack target of S-B1 is not a gas system measurement, intruders still need to inject false data into both power and gas system measurements to ensure the stealthiness of this FDIA. In addition, we observe that residuals after the FDIA become smaller than the residuals before the attack, as injected false data strictly follow operation constraints (B.1)-(B.6) without any noise. This observation is consistent with the

analysis in [18]. However, for SB-3, residual $\|\mathbf{r}\|$ soars and violates the threshold, since intruders do not consider the gas subsystem and ignore (11b). Consequently, this attack is detectable by IEGS BDD (10). Overall, this case validates i) the effectiveness of conditions (11) in designing (stealthy) FDIAs on IEGSs with complete network information, and ii) FDIAs on pure power systems cannot be applied to compromise the power subsystem in an IEGS due to the violation of (11b).

B. Integrated 39-Bus-Electricity-20-Node-Gas System

The IEGS-39-20 has ten generators (seven coal-fired generators and three gas-fired generators), two gas wells, nineteen power loads, and nine gas loads. See [29] for the detailed data.

1) *FDIAs on IEGSs with local network information.* This part tests conditions (15) for deriving *FDIAs on IEGSs with local network information*, and test results are presented in Table V. Intruders are assumed to have local network (topology and parameter) information of two areas, Area-1 (power buses 16, 19-24, and 33-36) and Area-2 (gas nodes 9-14 and 17-20), in the IEGS-39-20. (See [29] for the topology.) Measurement errors follow the same distribution as those in Scenario S-A1. Scen. S-C1 and S-C2 refer to different attack targets, i.e., voltage magnitude v_{23} in Area-1 and power and gas injections p_{36} and g_{17} in Area-1 and Area-2, respectively. According to test results, the FDIA in S-C1 incurs *fake thermal limit violations* due to reactive power flow increase (from -0.36 p.u. (before the FDIA) to -1.75 p.u. (after the FDIA) in the power transmission line connecting power buses 21 and 22), and the FDIA in S-C2 leads to *fake uneconomic dispatch*. See [29] for complete test data. Although both S-C1 and S-B1 aim to compromise a single voltage magnitude, the FDIA for S-C1 does not change any gas state, as Area-1 contains no gas-fired generators. Residuals $\|\mathbf{r}\|$ of S-C1 and S-C2 indicate conditions (15) are effective in designing FDIAs on IEGSs with incomplete network information.

TABLE V
FDIAs ON IEGSS WITH LOCAL NETWORK INFORMATION

Scen.	S-C1	S-C2
Attack target	v_{23}	p_{36} and g_{17}
Affected power state	$v_{21} - v_{24}, v_{35}, v_{36}, \theta_{21} - \theta_{24}, \theta_{35}, \theta_{36}$	$v_{19} - v_{24}, v_{33} - v_{36}, \theta_{19} - \theta_{24}, \theta_{33} - \theta_{36}$
Affected gas state	-	$c_{9,10}, \pi_9 - \pi_{11}, \pi_{17} - \pi_{20}$
Residual	1.1904	1.1904
$\ \mathbf{r}\ $	1.1904	1.1904

2) *FDIAs on IEGSs with only local topology information.* We test Proposition 1 for deriving *FDIAs on IEGSs with only local topology information*, and test results are shown in Table VI. Intruders are assumed to have only topology information of two local areas, i.e., Area-1 (power buses 16, 19-24, and 33-36) and Area-2 (gas nodes 9-14 and 17-20), in the IEGS-39-20. Particularly, in Area-2, gas nodes 9 and 10 are connected by two gas compressors, whose topology is the same as Case 3 in Fig. 2, and gas nodes 17 and 18, each with a gas load, are connected by one gas compressor, whose topology is the same as Case 2 in Fig. 2. Please refer to [29] for detailed topology. Measurement errors are set to be the same as those in Scenario S-C1. Scenarios S-D1 to S-D3 refer to different attack targets, i.e., voltage magnitude v_{23} in Area-1, gas injection g_{17} in Area-2, and gas flows in gas compressors $c'_{9,10}$ and $c''_{9,10}$ in Area-2, res-

pectively. For S-D1, we fail to find any feasible FDIA aiming at v_{23} for inducing voltage violation, and thus the residual A-R is not applicable (short for NA), numerically validating Lemma 1. For S-D2, intruders can launch an FDIA for compromising gas injection g_{17} . As is analyzed in Section IV.B (Lemma 2), this FDIA is an *gas load redistribution attack*, as it redistributes gas loads at gas nodes 17 and 18. For S-D3, there exists an FDIA aiming at gas flows in $c'_{9,10}$ and $c''_{9,10}$. As is analyzed in Section IV.B (Lemma 3), this FDIA is a *flow redistribution attack*, as it redistributes gas flows in two gas compressors {9, 10}. The above results verify Proposition 1 for deriving FDIAs on IEGSs with only local network topology information.

TABLE VI
FDIAs ON IEGSS WITH ONLY LOCAL TOPOLOGY INFORMATION

Scen.	S-D1	S-D2	S-D3
Attack target	v_{23}	g_{17}	$c_{9,10}$
Affected power state	-	-	-
Affected gas state	-	$c_{17,18}$	$c'_{9,10}, c''_{9,10}$
Affected IEGS measurements	-	$g_{17}, g_{18}, c_{17,18}$	$c'_{9,10}, c''_{9,10}$
Residual	1.1904	1.1904	1.1904
$\ \mathbf{r}\ $	NA	1.1904	1.1904

VI. CONCLUSION

This paper studies FDIAs on IEGSs with complete and incomplete network information. We consider the CAI and design FDIAs on IEGSs with complete network information. We also explain why previous FDIAs on pure power systems [6]-[8] cannot be applied to compromise the power subsystem of an IEGS. Then, for the first time, we develop i) FDIAs on IEGSs with local network (topology and parameter) information and ii) FDIAs on IEGSs with only local topology information. For the latter, we mathematically prove and numerically validate that: i) topology-only FDIAs on the power system of an IEGS cannot be devised in general, and ii) topology-only FDIAs on the gas system of an IEGS can be devised, specifically targeting gas compressors. Test results show that: i) coupling constraint (9b) is indispensable for IEGS SE; ii) IEGSs are vulnerable to FDIAs, even if intruders do not have complete network information; iii) IEGS operators should pay great attention to the cybersecurity of gas compressors. Future work includes detection, mitigation, and protection methods against FDIAs on IEGSs.

APPENDIX

In an IEGS, we have the following operation constraints.

$$p_{ij} = v_i^2 G_{ij} - v_i v_j [G_{ij} \cos(\theta_i - \theta_j) + B_{ij} \sin(\theta_i - \theta_j)], \quad \forall \{i, j\} \in \mathcal{P}_l, \quad (\text{B.1})$$

$$q_{ij} = -v_i^2 B_{ij} - v_i v_j [G_{ij} \sin(\theta_i - \theta_j) - B_{ij} \cos(\theta_i - \theta_j)], \quad \forall \{i, j\} \in \mathcal{P}_l, \quad (\text{B.2})$$

$$p_i = \sum_{j \in \mathcal{P}_l(i)} p_{ij}, \quad \forall i \in \mathcal{P}_n, \quad (\text{B.3})$$

$$q_i = \sum_{j \in \mathcal{P}_l(i)} q_{ij}, \quad \forall i \in \mathcal{P}_n, \quad (\text{B.4})$$

$$g_{ij} = \sqrt{W_{ij}(\pi_i^2 - \pi_j^2)}, \quad \forall \{i, j\} \in \mathcal{G}_l, \quad (\text{B.5})$$

$$g_i = \sum_{j \in \mathcal{G}_l(i)} g_{ij} + \sum_{j \in \mathcal{G}_c(i)} c_{ij}, \quad \forall i \in \mathcal{G}_n. \quad (\text{B.6})$$

Constraints (B.1) and (B.2) determine real and reactive power

flow in power transmission line $\{i, j\}$, respectively. Constraints (B.3) and (B.4) denote real and reactive power injections at power bus i , respectively. Set $\mathcal{P}_{l(i)}$ is composed of power buses connected to power bus i via power transmission line l . Constraint (B.5) is the unidirectional Weymouth equation [9]-[12], [26], which simulates the gas flow in gas passive pipeline $\{i, j\}$. Constraint (B.6) is the gas injection at gas node i . Sets $\mathcal{G}_{l(i)}$ and $\mathcal{G}_{c(i)}$ consist of gas nodes connected to gas node i via gas passive pipelines and gas compressors, respectively. Note that different from AC power flows, where $p_{ij} \neq -p_{ji}$ and $q_{ij} \neq -q_{ji}$ in general, gas flows $g_{ij} = -g_{ji}$ and $c_{ij} = -c_{ji}$. In other words, we do not consider line pack, as the scope of this paper is static SE. Real and reactive power injections and gas injections are derived by

$$p_i = \sum_{g \in \mathcal{P}_{g(i)} \cup \mathcal{G}_{g(i)}} p_g - \sum_{d \in \mathcal{P}_{d(i)}} P_d, \quad \forall i \in \mathcal{P}_n, \quad (\text{B.7})$$

$$q_i = \sum_{g \in \mathcal{P}_{g(i)} \cup \mathcal{G}_{g(i)}} q_g - \sum_{d \in \mathcal{P}_{d(i)}} Q_d, \quad \forall i \in \mathcal{P}_n, \quad (\text{B.8})$$

$$g_i = \sum_{w \in \mathcal{G}_{w(i)}} g_w - \sum_{d \in \mathcal{G}_{d(i)}} G_d - \sum_{g \in \mathcal{G}_{g(i)}} \gamma_g P_g, \quad \forall i \in \mathcal{G}_n. \quad (\text{B.9})$$

Sets $\mathcal{P}_{g(i)}$, $\mathcal{G}_{g(i)}$, and $\mathcal{P}_{d(i)}$ consist of coal-fired power generators, gas-fired power generators, and power loads connected to power bus i , respectively. Sets $\mathcal{G}_{w(i)}$ and $\mathcal{G}_{d(i)}$ are composed of gas wells and gas loads connected to gas node i , respectively. Particularly, constraint (B.9) reflects the interdependency between power and gas systems in an IEGS. Although constraint (B.9) assumes that each gas-fired power generator is supplied by one gas node, it can be extended to general cases, i.e., one gas-fired generator supplied by multiple gas nodes.

If there exist (at least) one pair of power bus i and gas node j in an IEGS that satisfies A.i) power bus i connects only one gas-fired power generator, A.ii) this generator is supplied by gas node j , and A.iii) gas node j has no gas wells or gas loads (except for the gas-fired generator), we have

$$g_j = \gamma_g p_i, \quad \forall g \in \mathcal{G}_{g(i)}, \quad \{i, j\} \in \mathcal{C}_n, \quad (\text{B.10})$$

i.e., the coupling constraint in an IEGS, where \mathcal{C}_n is the set of pairs of power buses and gas nodes satisfying A.i)-A.iii).

REFERENCES

- [1] U.S. Energy Information Administration (EIA), Annual Energy Review, 2021 [Online]. Available: <https://www.eia.gov/totalenergy/data/annual/>
- [2] National Statistics, Energy Trends: UK Electricity, 2021 [Online]. Available: <https://www.gov.uk/government/statistics/electricity-section-5-energy-trends>
- [3] International Energy Agency (IEA), Power Systems in Transition: Challenges and Opportunities Ahead for Electricity Security, 2020 [Online]. Available: <https://www.iea.org/reports/power-systems-in-transition/cyberresilience>
- [4] United States Government Accountability Office (GAO), Electricity Grid Cybersecurity: DOE Needs to Ensure Its Plans Fully Address Risks to Distribution Systems, 2021, [Online]. Available: <https://www.gao.gov/products/gao-21-81>
- [5] U.S. Department of Energy (DoE), Colonial Pipeline Cyber Incident, 2021 [Online]. Available: <https://www.energy.gov/ceser/colonial-pipeline-cyber-incident>
- [6] Y. Liu, P. Ning, and M. K. Reiter, "False data injection attacks against state estimation in electric power grids," *ACM Trans. Inf. Syst. Security*, vol. 14, no. 1, May 2011, Art. no. 13.
- [7] G. Hug and J. A. Giampapa, "Vulnerability assessment of AC state estimation with respect to false data injection cyber-attacks," *IEEE Trans. Smart Grid*, vol. 3, no. 3, pp. 1362-1370, Sept. 2012.
- [8] P. Zhuang and H. Liang, "False data injection attacks against state-of-charge estimation of battery energy storage systems in smart distribution networks," *IEEE Trans. Smart Grid*, vol. 12, no. 3, pp. 2566-2577, May 2021.
- [9] B. Zhao, A. J. Lamadrid, R. S. Blum, and S. Kishore, "A coordinated scheme of electricity-gas systems and impacts of a gas system FDI attacks on electricity system," *Int. J. Electr. Power Energy Syst.*, vol. 131, p. 107060, Oct. 2021.
- [10] B. Zhao, A. J. Lamadrid, R. S. Blum, and S. Kishore, "A trilevel model against false gas-supply information attacks in electricity systems," *Elect. Power Syst. Res.*, vol. 189, p. 106541, 2020.
- [11] I. L. Carreño, A. Scaglione, A. Zlotnik, D. Deka, and K. Sundar, "An adversarial model for attack vector vulnerability analysis on power and gas delivery operations," *Elect. Power Syst. Res.*, vol. 189, p. 106777, 2020.
- [12] M. Zadsar, A. Abazari, A. Ameli, J. Yan, and M. Ghafouri, "Prevention and detection of coordinated false data injection attacks on integrated power and gas systems," *IEEE Trans. Power Syst.*, 2022 (in press).
- [13] P. Zhao *et al.*, "Cyber-resilient multi-energy management for complex systems," *IEEE Trans. Ind. Informat.*, vol. 18, no. 3, pp. 2144-2159, March 2022.
- [14] P. Zhao, C. Gu, and D. Huo, "Coordinated risk mitigation strategy for integrated energy systems under cyber-attacks," *IEEE Trans. Power Syst.*, vol. 35, no. 5, pp. 4014-4025, Sept. 2020.
- [15] P. Zhao *et al.*, "A cyber-secured operation for water-energy nexus," *IEEE Trans. Power Syst.*, vol. 36, no. 4, pp. 3105-3117, July 2021.
- [16] X. Liu and Z. Li, "Local load redistribution attacks in power systems with incomplete network information," *IEEE Trans. Smart Grid*, vol. 5, no. 4, pp. 1665-1676, July 2014.
- [17] X. Liu, Z. Bao, D. Lu, and Z. Li, "Modeling of local false data injection attacks with reduced network information," *IEEE Trans. Smart Grid*, vol. 6, no. 4, pp. 1686-1696, July 2015.
- [18] X. Liu and Z. Li, "False data attacks against AC state estimation with incomplete network information," *IEEE Trans. Smart Grid*, vol. 8, no. 5, pp. 2239-2248, Sept. 2017.
- [19] R. Deng, P. Zhuang, and H. Liang, "False data injection attacks against state estimation in power distribution systems," *IEEE Trans. Smart Grid*, vol. 10, no. 3, pp. 2871-2881, May 2019.
- [20] S. Bi and Y. J. Zhang, "Using covert topological information for defense against malicious attacks on DC state estimation," *IEEE J. Sel. Areas Commun.*, vol. 32, no. 7, pp. 1471-1485, July 2014.
- [21] A. Tajer, "False data injection attacks in electricity markets by limited adversaries: stochastic robustness," *IEEE Trans. Smart Grid*, vol. 10, no. 1, pp. 128-138, Jan. 2019.
- [22] W.-L. Chin, C.-H. Lee, and T. Jiang, "Blind false data attacks against AC state estimation based on geometric approach in smart grid communications," *IEEE Trans. Smart Grid*, vol. 9, no. 6, pp. 6298-6306, Nov. 2018.
- [23] Y. Song, X. Liu, Z. Li, M. Shahidehpour, and Z. Li, "Intelligent data attacks against power systems using incomplete network information: a review," *J. Mod. Power Syst. Clean Energy*, vol. 6, no. 4, pp. 630-641, July 2018.
- [24] National Renewable Energy Lab (NREL), Electric Power Grid and Natural Gas Network Operations and Coordination, 2021 [Online]. Available: <https://www.nrel.gov/docs/fy20osti/77096.pdf>.
- [25] T. W. K. Mak, P. V. Hentenryck, A. Zlotnik, and R. Bent, "Dynamic compressor optimization in natural gas pipeline systems," *Inform. J. Comput.*, vol. 31, no. 1, pp. 40-65, Jan. 2019.
- [26] Z. Wang and R. S. Blum, "Elimination of undetectable attacks on natural gas networks," *IEEE Signal Process. Lett.*, vol. 28, pp. 1002-1005, 2021.
- [27] W. Zheng, W. Wu, A. Gomez-Exposito, B. Zhang, and Y. Guo, "Distributed robust bilinear state estimation for power systems with nonlinear measurements," *IEEE Trans. Power Syst.*, vol. 32, no. 1, pp. 499-509, Jan. 2017.
- [28] J. Zhao, L. Mili, and M. Wang, "A generalized false data injection attacks against power system nonlinear state estimator and countermeasures," *IEEE Trans. Power Syst.*, vol. 33, no. 5, pp. 4868-4877, Sep. 2018.
- [29] [Online]. Available: <https://sites.google.com/site/rongpengliu1991/>
- [30] R.-P. Liu, Y. Hou, Y. Li, S. Lei, W. Wei, and X. Wang, "Sample robust scheduling of electricity-gas systems under wind power uncertainty," *IEEE Trans. Power Syst.*, vol. 36, no. 6, pp. 5889-5900, Nov. 2021.
- [31] L. Yang, Y. Xu, W. Gu, and H. Sun, "Distributionally robust chance-constrained optimal power-gas flow under bidirectional interactions considering uncertain wind power," *IEEE Trans. Smart Grid*, vol. 12, no. 2, pp. 1722-1735, March 2021.
- [32] X. Liu, Z. Bao, D. Lu, and Z. Li, "Modeling of local false data injection attacks with reduced network information," *IEEE Trans. Smart Grid*, vol. 6, no. 4, pp. 1686-1696, July 2015.

SUPPLEMENTARY MATERIALS

Rong-Peng Liu, Xiaozhe Wang, Zuyi Li, and Rawad Zgheib

Note that all the equation numbers and reference numbers starting with an ‘‘R’’ refer to those introduced in this document, and the equation numbers and reference numbers starting with a ‘‘number’’ or ‘‘B’’ refer to those introduced in the paper.

A. Analysis When Intruders Does not Have the Same Estimated States as Those Estimated by IEGS Operators

Without loss of generality, let $\hat{\mathbf{x}}' = \hat{\mathbf{x}} + \xi$, where ξ is the *bias* between $\hat{\mathbf{x}}'$, the vector of estimated states by intruders, and $\hat{\mathbf{x}}$, the vector of estimated states by IEGS operators. Next, we analyze the impact of bias on the stealthiness of FDIAs on IEGSs (by observing residuals \mathbf{r}_{bad} and $\mathbf{r}_{\text{c, bad}}$). Since intruders do not know the existence or the exact value of the bias in their estimated states, they routinely employ conditions (R17)-(R18) to design an FDIA, i.e.,

$$\Delta \mathbf{z} = \mathbf{h}(\hat{\mathbf{x}} + \xi + \Delta \mathbf{x}) - \mathbf{h}(\hat{\mathbf{x}} + \xi), \quad (\text{R17})$$

$$\|\mathbf{T} \cdot \mathbf{h}_c^p(\hat{\mathbf{x}}^p + \xi^p + \Delta \mathbf{x}^p) - \mathbf{h}_c^g(\hat{\mathbf{x}}^g + \xi^g + \Delta \mathbf{x}^g)\| \leq \epsilon_{\text{bad}}, \quad (\text{R18})$$

where $\xi = \text{col}(\xi^p, \xi^g)$. Then, IEGS operators conduct BDD by examining $\|\mathbf{r}_{\text{bad}}\|$ and $\|\mathbf{r}_{\text{c, bad}}\|$ in (10). For $\|\mathbf{r}_{\text{bad}}\|$, we have

$$\begin{aligned} \|\mathbf{r}_{\text{bad}}\| &= \|\mathbf{z}_{\text{bad}} - \mathbf{h}(\mathbf{x}_{\text{bad}})\| \\ &= \|\mathbf{z} + \Delta \mathbf{z} - \mathbf{h}(\hat{\mathbf{x}} + \Delta \mathbf{x})\| \\ &= \|\mathbf{z} - \mathbf{h}(\hat{\mathbf{x}}) + \mathbf{h}(\hat{\mathbf{x}} + \xi + \Delta \mathbf{x}) - \mathbf{h}(\hat{\mathbf{x}} + \xi) + \mathbf{h}(\hat{\mathbf{x}}) - \mathbf{h}(\hat{\mathbf{x}} + \Delta \mathbf{x})\| \\ &= \|\mathbf{r} + (\mathbf{h}(\hat{\mathbf{x}} + \Delta \mathbf{x} + \xi) - \mathbf{h}(\hat{\mathbf{x}} + \Delta \mathbf{x})) - (\mathbf{h}(\hat{\mathbf{x}} + \xi) - \mathbf{h}(\hat{\mathbf{x}}))\|. \end{aligned} \quad (\text{R19})$$

Equation (R19) quantitatively analyzes the impact of bias ξ on residuals \mathbf{r}_{bad} . This enables intruders to *exactly* evaluate the stealthiness of any FDIA under different biases. Particularly, when ξ is small, i.e., intruders have confidence in their estimated states, we have

$$\begin{aligned} \|\mathbf{r}_{\text{bad}}\| &= \|\mathbf{r} + (\mathbf{h}(\hat{\mathbf{x}} + \Delta \mathbf{x} + \xi) - \mathbf{h}(\hat{\mathbf{x}} + \Delta \mathbf{x})) - (\mathbf{h}(\hat{\mathbf{x}} + \xi) - \mathbf{h}(\hat{\mathbf{x}}))\| \\ &= \|\mathbf{r} + (\mathbf{J}_1 - \mathbf{J}_2) \cdot \xi + o(\xi)\| \\ &\approx \|\mathbf{r} + (\mathbf{J}_1 - \mathbf{J}_2) \cdot \xi\| \\ &\leq \|\mathbf{r}\| + \|(\mathbf{J}_1 - \mathbf{J}_2)\| \|\xi\|, \end{aligned} \quad (\text{R20})$$

an *approximate upper bound* for the FDIAs on IEGSs. $\mathbf{J}_1 = \partial \mathbf{h} / \partial \mathbf{x}|_{\mathbf{x} = \hat{\mathbf{x}} + \Delta \mathbf{x}}$ and $\mathbf{J}_2 = \partial \mathbf{h} / \partial \mathbf{x}|_{\mathbf{x} = \hat{\mathbf{x}}}$ are constant matrices. The second line in (R20) is derived by the Taylor expansion, and the third line is an approximation by neglecting higher-order terms of ξ , as ξ is assumed to be small. If this bound is no larger than τ , we have $\|\mathbf{r}_{\text{bad}}\| \leq \tau$, i.e., the residuals \mathbf{r}_{bad} can bypass BDD. Note that the last line in (R20) indicates that the upper bound of $\|\mathbf{r}_{\text{bad}}\|$ varies affinely with bias ξ . This affine relation allows intruders to easily extrapolate how the variation of a bias affects residual $\|\mathbf{r}_{\text{bad}}\|$, so as to evaluate the stealthiness of an FDIA.

Different from \mathbf{r}_{bad} , the BDD for $\mathbf{r}_{\text{c, bad}}$ only allows a very small numerical error (e.g., $\epsilon_{\text{bad}} = 1e^{-5}$). Any bias in estimated states $\hat{\mathbf{x}}'$ may result in the violation of (R18), i.e., $\|\mathbf{r}_{\text{c, bad}}\| = \|\mathbf{T} \cdot \mathbf{h}_c^p(\hat{\mathbf{x}}^p + \Delta \mathbf{x}^p) - \mathbf{h}_c^g(\hat{\mathbf{x}}^g + \Delta \mathbf{x}^g)\| > \epsilon_{\text{bad}}$, as the FDIA is designed based on (R17)-(R18). In order to enable $\mathbf{r}_{\text{c, bad}}$ to bypass BDD, intruders should manage to ensure the accurate estimation for the state variables \mathbf{x} in (B.10)², i.e.,

$$\mathbf{A}^p \cdot \xi^p = 0, \mathbf{A}^g \cdot \xi^g = 0, \quad (\text{R21})$$

where \mathbf{A}^p and \mathbf{A}^g are coefficient matrices, which enable $\mathbf{A}^p \cdot \xi^p$ and $\mathbf{A}^g \cdot \xi^g$ to denote the errors of the estimated power and gas system states in (B.10), respectively. For this case, we have $\|\mathbf{r}_{\text{c, bad}}\| = \|\mathbf{T} \cdot \mathbf{h}_c^p(\hat{\mathbf{x}}^p + \xi^p + \mathbf{x}^p) - \mathbf{h}_c^g(\hat{\mathbf{x}}^g + \xi^g + \Delta \mathbf{x}^g)\| = \|\mathbf{T} \cdot \mathbf{h}_c^p(\hat{\mathbf{x}}^p + \Delta \mathbf{x}^p) - \mathbf{h}_c^g(\hat{\mathbf{x}}^g + \Delta \mathbf{x}^g)\| \leq \epsilon_{\text{bad}}$, indicating residuals $\mathbf{r}_{\text{c, bad}}$ can bypass BDD. In practice, condition (R21) is elusive, as intruders hardly know exact biases. Another method is to keep the estimation of the state variables in (B.10) unchanged (before and after an FDIA), i.e.,

$$\mathbf{A}^p \cdot \Delta \mathbf{x}^p = 0, \mathbf{A}^g \cdot \Delta \mathbf{x}^g = 0. \quad (\text{R22})$$

In this case, intruders employ (R22) for keeping relevant estimated states the same. Thus, $\|\mathbf{r}_{\text{c, bad}}\| = \|\mathbf{T} \cdot \mathbf{h}_c^p(\hat{\mathbf{x}}^p + \Delta \mathbf{x}^p) - \mathbf{h}_c^g(\hat{\mathbf{x}}^g + \Delta \mathbf{x}^g)\| = \|\mathbf{T} \cdot \mathbf{h}_c^p(\hat{\mathbf{x}}^p) - \mathbf{h}_c^g(\hat{\mathbf{x}}^g)\| = 0 \leq \epsilon_{\text{bad}}$, i.e., residuals $\mathbf{r}_{\text{c, bad}}$ can bypass BDD.

² The state variables in (B.10) refer to the state variables \mathbf{x} that are related to the power and gas injections in (B.10) (via (B.1), (B.2), (B.5), and (B.6)).

B. Detailed Compressor Model

For a compressor that connects gas nodes i and j (with a flow direction from i to j), the detailed model [28] is

$$\rho_i = \pi_i / (\mathbf{R}_s \mathbf{T} u_i), \quad (\text{R23})$$

$$u_i = 1 + 0.257(\pi_i / \pi_c) - 0.533(\mathbf{T}_c / \mathbf{T})(\pi_i / \pi_c), \quad (\text{R24})$$

$$v_{ij} = c_{ij} / \rho_i, \quad (\text{R25})$$

$$h_{ij} = \mathbf{R}_s \mathbf{T} (\kappa / (\kappa - 1)) \left((\pi_j / \pi_i)^{\kappa - 1 / \kappa} - 1 \right) u_i, \quad (\text{R26})$$

$$P_{c_ij} = c_{ij} h_{ij} / \eta_{ij}, \quad (\text{R27})$$

$$b_{ij} = f_1(P_{c_ij}; \mathbf{a}_1), \quad (\text{R28})$$

$$P_{c_ij} \leq P_{c_ij}, \quad (\text{R29})$$

$$P_{c_ij} = f_2(n_{ij}, \mathbf{T}_a; \mathbf{A}_1), \quad (\text{R30})$$

$$h_{ij} = f_2(v_{ij}, n_{ij}; \mathbf{A}_2), \quad (\text{R31})$$

$$\eta_{ij} = f_2(v_{ij}, n_{ij}; \mathbf{A}_3), \quad (\text{R32})$$

$$f_1(v_{ij}; \mathbf{a}_2) \leq h_{ij} \leq f_1(v_{ij}; \mathbf{a}_3), \quad (\text{R33})$$

$$\mathbf{N}_{ij}^{\min} \leq n_{ij} \leq \mathbf{N}_{ij}^{\max}, \quad (\text{R34})$$

$$n_{ij} = v_{ij} / \mathbf{V}_0, \quad (\text{R35})$$

$$m_{ij} = (\mathbf{V}_0 h_{ij} / (2\pi \eta_{ij})) \rho_i, \quad \eta_{ij} = \bar{\eta}_{ij}. \quad (\text{R36})$$

\mathbf{a}_1 , \mathbf{a}_2 , and \mathbf{a}_3 are constant (3×1) vectors, and \mathbf{A}_1 , \mathbf{A}_2 , and \mathbf{A}_3 are constant (3×3) matrices. $f_1(x; \mathbf{a}_1) = a_{12}x^2 + a_{11}x + a_{10}$, and $f_2(x, y; \mathbf{A}_1) = [x^2 \ x \ 1] \mathbf{A}_1 [y^2 \ y \ 1]^T$, where $\mathbf{a}_1 = \text{col}(a_{12}, a_{11}, a_{10})$. Please refer to Table RI for detailed descriptions about parameters and variables. Since this paper focuses on single-period FDIAs launched within a short time, we set \mathbf{T} , \mathbf{T}_c , and \mathbf{T}_a as constants. Constraint (R23) is the thermodynamical standard equation. Constraint (R24) indicates the relation between the compressibility factor and gas nodal pressure. Constraint (R25) transforms mass gas flow into volumetric gas flow. Constraint (R26) shows how the gas nodal pressure and compressibility factor affect the adiabatic enthalpy. Constraints (R27) and (R28) calculate the input power of a compressor and its energy consumption rate, respectively. Constraints (R29) and (R30) regulate the compressor input power limit. Constraints (R31)-(R34) and (R34)-(R36) model turbo and piston compressors, respectively. For a turbo compressor, constraints (R31) and (R32) give the compressor speed and adiabatic efficiency, respectively, and constraints (R33) and (R34) enforce the ranges of the adiabatic enthalpy change and compressor speed, respectively. For a piston compressor, constraints (R35) and (R36) define the compressor speed and shaft torque, respectively. Note that the adiabatic efficiency in a piston compressor is set as a constant [28]. (See (R36).) Here, we assume constraint (R31) has at least one feasible n_{ij} with any (fixed) v_{ij} and h_{ij} .

If we do not increase the number of measurements, then the measurements for a detailed compressor are c_{ij} , $\{i, j\} \in \mathcal{G}_c$, and π_i , $i \in \mathcal{G}_n$. For this case, we define the state variables for turbo and piston compressors as \mathbf{x}_T^g and \mathbf{x}_P^g , respectively, where $\mathbf{x}_T^g = \text{col}(\rho_i, u_i, v_{ij}, h_{ij}, P_{c_ij}, \eta_{ij}, b_{ij}, n_{ij}, P_{c_ij})$ and $\mathbf{x}_P^g = \text{col}(\rho_i, u_i, v_{ij}, h_{ij}, P_{c_ij}, \eta_{ij}, b_{ij}, n_{ij}, P_{c_ij}, m_{ij})$, $i \in \mathcal{G}_n$, $\{i, j\} \in \mathcal{G}_c$. When all measurements c_{ij} and π_i are fixed, the values of \mathbf{x}_T^g and \mathbf{x}_P^g are uniquely determined by (R23)-(R34) and (R23)-(R30), (R34)-(R36), respectively. That means the IEGSs with either detailed compressor model or both are observable. Thus, a plausible SE paradigm (for IEGSs with detailed compressor models) is to i) employ (9) (without any changes) for deriving estimated IEGS states $\hat{\mathbf{x}}$; ii) calculate estimated measurements $h(\hat{\mathbf{x}})$; iii) leverage estimated measurements $h(\hat{\mathbf{x}})$ to estimate \mathbf{x}_T^g and \mathbf{x}_P^g (by (R23)-(R36)). For this IEGS SE, intruders can still launch FDIAs by following (11) (without any changes). Namely, the FDIAs developed in Section III.A also applies to IEGSs with detailed compressor models.

TABLE RI
COMPRESSOR PARAMETERS AND VARIABLES

Parameter	Description	Parameter	Description
R_s	Gas constant	T_a	Ambient temperature
T	Temperature	$N_{ij}^{\min/\max}$	Compressor speed limit
π_c	Pseudocritical pressure	V_0	Operating volume
T_c	Gas temperature	$\bar{\eta}_{ij}$	Constant adiabatic efficiency
κ	Isentropic exponent		
Variable	Description	Variable	Description
ρ_i	Gas density	η_{ij}	Adiabatic efficiency
u_i	Compressibility factor	b_{ij}	Energy consumption rate
v_{ij}	Volumetric gas flow rate	n_{ij}	Compressor speed
h_{ij}	Adiabatic enthalpy change	$P_{c,ij}$	Maximum input power
$P_{c,ij}$	Compressor input power	m_{ij}	Shaft torque

C. Power-to-Gas (P2G) Facilities

IEGSs may include P2G facilities [33]. These facilities are able to transform (surplus) electricity into natural gas. Similar to gas-fired generators, P2G facilities introduce coupling relations to IEGSs. For accurate state estimation of P2G facility-embedded IEGSs, system operators should add constraint (R37) to (10b):

$$g_j = \chi_f p_i, \forall f \in \mathcal{G}_{f(i)}, \{i, j\} \in \mathcal{F}_n, \quad (\text{R37})$$

where χ_f is the electricity-gas conversion ratio of P2G facility f , $\mathcal{G}_{f(i)}$ is the set of the P2G facilities connected to power bus i , and \mathcal{F}_n is the set of pairs of power bus i and gas node j that satisfy: i) power bus i only connects a P2G facility (i.e., power bus i does not have any power generator or power load), ii) this P2G facility transmits natural gas to gas node j , and iii) gas node j only connects this P2G facility (i.e., gas node j does not have any gas wells or gas load). Constraint (R37) guarantees that the estimated natural gas output of P2G facilities do not contradict the power consumption. Accordingly, the BDD, FDIAs, and impact analysis of bias can be smoothly implemented by simply using (10), (11), and (R17)-(R20), respectively.